Assessing Berry Number for Grapevine Yield Estimation by Image Analysis: Case Study with the Red Variety “Syrah”

Giorgia Attinà

Dissertation to obtain a Master’s Degree in

Bologna Master Degree in Viticulture and Enology Engineering

Supervisor: Carlos Manuel Antunes Lopes

Co-Supervisor: Vittorino Novello

Jury:

President: PhD Joaquim Miguel Rangel da Cunha Costa, Assistant Professor at Instituto Superior de Agronomia, Universidade de Lisboa.

Members: PhD Carlos Manuel Antunes Lopes, Associate Professor with Habilitation at Instituto Superior de Agronomia, Universidade de Lisboa;

PhD Ricardo Nuno da Fonseca Garcia Pereira Braga, Assistant Professor at Instituto Superior de Agronomia, Universidade de Lisboa.

2020

ACNOWLEDGEMENT

First, I would like to acknowledgement my supervisor Professor Carlos Lopes for his knowledge, patient and priceless support for this project.

I would like to express my sincere grateful to Gonçalo Victorino for his help and support.

I also would like to thank my Italian supervisor Professor Vittorino Novello for his availability and kind supervision.

Thank to Sergio and Peppe for the encouragement and helping each other throughout the period of the dissertation. Big team!

Thank to new and old friends for their support throughout these years, including lockdowns. You have been instrumental in achieving this goal.

Thank to Asti and Lisbon where I met my colleagues and now especially fantastic friends with whom I shared one of the most beautiful periods of my life. It is true that friends are the family you choose.

Finally, I would like to thank with all my heart my family, especially my mother Roberta, my father Albino and my sister, friend and colleague Letizia. Thank you to have always believed in me more than I believed in myself and to be my models of life. You always have been close to me, in good and bad times, in moment of joy and discouragement. I dedicate my thesis to you. I love you.

ABSTRACT

The yield estimation provides information that help growers to make decisions in order to optimize crop growth and to organize the harvest operations in field and in the cellar. In most vineyard estates yield is forecasted using manual methods. However, image analysis methods, which are less invasive low cost and more representative are now being developed. The main objective of this work was to estimate yield through data obtained in the frame of Vinbot project during the 2019 season. In this thesis, images of the grapevine variety Syrah taken in the laboratory and in the vineyards of the “Instituto Superior de Agronomia” in Lisbon were analyzed. In the laboratory the images were taken manually with an RGB camera, while in the field vines were imaged either manually and by the Vinbot robot. From these images, the number of visible berries were counted with MATLAB. From the laboratory values, the relationships between the number of visible berries and actual bunch weight and berry number were studied. From the data obtained in the field, it was analyzed the visibility of the berries at different levels of defoliation and the relationship between the area of visible bunches and the visible berries. Berry-by-berry occlusion showed a value of 6.4% at pea-size, 14.5% at veraison and 25% at maturation. In addition, high and significant determination coefficient were obtained between actual yield and visible berries. The comparison of estimated yield, obtained using the regression models with actual yield, showed an underestimation at all the three phonological stages. This low accuracy of the developed models show that the use of algorithms based on visible berry number on the images to estimate yield still needs further research.

Keyword: Yield estimation, algorithm, precision viticulture, image analysis, Vinbot.

RESUMO

A estimativa da produção fornece informações que auxiliam os produtores a otimizar o crescimento da cultura e a organizar a vindima. Na maioria das empresas vitícolas, o rendimento é estimado usando métodos manuais. No entanto, métodos de análise de imagem que são menos invasivos, de baixo custo e mais representativos estão sendo desenvolvidos. O principal objetivo deste trabalho é estimar a produtividade por meio de dados obtidos no âmbito do projeto Vinbot durante o ciclo de 2019. Foram analisadas imagens da casta Syrah tiradas em laboratório e nas vinhas do Instituto Superior de Agronomia de Lisboa. No laboratório as imagens foram tiradas manualmente com uma câmera RGB, enquanto no campo as videiras foram fotografadas quer manualmente quer usando o robô Vinbot. O número de bagos visíveis obtidos a partir destas imagens foram correlacionados com o peso real do cacho e com o rendimento em três estados fenológicos. A partir dos valores de laboratório, foram estudadas as relações entre o número de bagos visíveis e o peso real do cacho e o número de bagos. A partir dos dados obtidos no campo, foi analisada a visibilidade dos bagos em diferentes níveis de desfolha e a relação entre a área dos cachos visíveis e os bagos visíveis. A oclusão bago por bago apresentou um valor de 6,4% ao bago de ervilha, 14,5% no pintor e 25% na maturação. Obtiveram-se elevados e significativos coeficientes de determinação na análise de regressão entre a produção real e o número de bagos visíveis. A comparação da produtividade estimada pelos modelos de regressão, com a produtividade real, apresentou uma subestimação em todas as fases fenológicas. Esta baixa precisão dos modelos desenvolvidos mostra que o uso de algoritmos baseados no número de bagos visíveis nas imagens para estimar o rendimento ainda precisa de ser mais estudado.

Palavra-chave: Estimativa de rendimento, algoritmo, viticultura de precisão, análise de imagem, Vinbot.

RESUMO ALARGADO

A estimativa de rendimento representa a previsão do potencial de produção da vinha. Fornece informações sobre as medidas a serem tomadas, a fim de otimizar o crescimento da cultura e organizar a operação de colheita no campo e na adega. O principal objetivo da viticultura de precisão é minimizar os custos de produção e, entretanto, melhorar a qualidade da colheita, garantindo a preservação do meio ambiente. Nos últimos anos, a estimativa do rendimento tornou-se um dos tópicos importantes da viticultura. Os métodos atuais para estimar o rendimento são trabalhosos, destrutivos, imprecisos e caros. Na verdade, o tamanho da amostra é frequentemente muito pequeno em comparação com a variabilidade espacial de um vinhedo, portanto, as estimativas de produção serão imprecisas. A previsão clássica da produção é obtida através do conhecimento de dados históricos ou de medições feitas manualmente na vinha. Normalmente, o rendimento é previsto com métodos manuais. No entanto, com o objetivo de melhorar a estimativa de rendimento, métodos baseados em análise de imagem, que são menos invasivos, de baixo custo e mais representativos estão a ser estudados. Além disso, outras tecnologias inovadoras foram desenvolvidas na agricultura, por exemplo, o robô VINBOT que é uma nova plataforma terrestre capaz de estimar o rendimento através da metodologia de análise de imagens. O principal objetivo deste trabalho é estimar a produtividade por meio de dados obtidos no âmbito do projecto Vinbot durante o ano de 2019. Nesta dissertação, foram analisadas imagens da casta Syrah, colhidas em laboratório e em vinhas do Instituto Superior de Agronomia, Lisboa. No laboratório as imagens foram tiradas manualmente com uma câmera RGB, enquanto no campo as videiras foram fotografadas quer manualmente quer usando o robô Vinbot. O número de bagos visíveis obtidos a partir destas imagens foram correlacionados com o peso real do cacho e com o rendimento em três estados fenológicos (bago de ervilha, pintor e maturação). A partir dos valores de laboratório, foram estudadas as relações entre o número de bagos visíveis e o peso real do cacho e o número de bagos. A partir dos dados obtidos no campo, foi analisada a visibilidade dos bagos em diferentes níveis de desfolha e a relação entre a área dos cachos visíveis e os bagos visíveis. A oclusão bago por bago apresentou um valor de 6,4% ao bago de ervilha, 14,5% no pintor e 25% na maturação. Obtiveram-se elevados e significativos coeficientes de determinação (R2 = 0,60 ** ao bago de ervilha, R2 = 0,68 *** na fase de pintor e R2 = 0,61 ** na maturação) na análise de regressão entre a produção real e o número de bagos visíveis. Finalmente, a produtividade foi estimada usando modelos de regressão baseados na relação entre a porosidade da sebe e o número de bagos, combinados com os valores do peso do bago

determinado em laboratório à vindima. Em seguida, a estimativa do rendimento foi comparada com o valor real, obtendo-se um erro de -51% ao bago de ervilha, -33,3% ao pintor e -37,8% à maturação. Conclui-se que, apesar da estimativa do rendimento poder ser obtida através destas técnicas de análise de imagem, a baixa precisão dos modelos desenvolvidos indicam que o uso de algoritmos baseados no número de bagos visíveis nas imagens ainda é uma metodologia que precisa de ser mais estudada.

Palavra-chave: Estimativa de rendimento, algoritmo, viticultura de precisão, análise de imagem, Vinbot.

INDEX

LIST OF TABLES

LIST OF FIGURES

LIST OF EQUATIONS

LIST OF ABBREVIATIONS

2D two-dimensional

3D three-dimensional

a* greenness-redness coordinate

AbO_B berry-by-berry occlusion measured at bunch level

ABV actual bunch volume

AbW average berry weight

APFM Aeropalynological Forecast Model

b* blueness-yellowness coordinate

btot. total number of visible berries without berries and leaves occlusion

bW berry weight

BW bunch weight

CCD Charge Coupled Device

CIE Commission International d' Eclairage

CIElab Color space CIE L*a*b*

CNN Convolutional Neural Network

E error between actual and estimated yield

F1 harmonic average between Recall and Precision

FCN Fully Convolutional Network

GBCNet Grape Berries Counting Net

GIS Geographic Information System

GPS Global Position System

HMI Human Machine Interface

HSB Hue, Saturation, Brightness

IF Fruitfulness index

IPMA Instituto Português do Mar e da Atmosfera

ISA Instituto Superior de Agronomia

L* Luminance coordinate

LAI Leaf Area Index

LIDAR Light Detection and Ranging or Laser Imaging Detection and Ranging

NDVI Normalized Difference Vegetation Index

NIR Near-Infrared Spectroscopy

NN Artificial Neural Networks

OIV International Organization of Vine and Wine

P canopy porosity

PV Precision Viticulture

RGB Red, Green, Blue

ROI Region of Interest

SLAM Simultaneous Localization And Mapping

SMPH Semi Minimal Pruned Hedge

SP Smart Point

SVM Support Vector Machines

Tt,a trellis wire tension at the time t from the antecedent year

Tt,c trellis wire tension at time t of the current year.

Tb_L number of total berries measured in laboratory

TTM Trellis Tension Method

UAV Unmanned Aerial Vehicle

VBA visible bunch area

Vb_B Visible berries measured at bunch level

Vb_L visible berries in laboratory condition

Vb_v Visible berries measured at vine level

Vbtot total number of visible berries without leaves occlusion

VSP Vertical Shoot Position

WSN Wireless Sensor Network

Y actual yield

Ya yield from an antecedent year.

Yt,c yield predicted at any time (t) of the current year

Yest estimated yield

1. INTRODUCTION

The yield estimation represents the forecast of the vineyard winegrape potential (Diago et al., 2012). It is an important point for any wine industry because it allows to improve the management of vineyards and to obtain the desired wine quality (Diago et al., 2012; Liu et al., 2013). In fact, it provides information about the measures to be taken, with the aim to optimize crop growth monitoring and to organize the harvest operation (Nuske et al., 2011a; Diago et al., 2012; Liu et al., 2013; Aquino et al., 2018b). The yield forecasting is also important from an economic point of view, as it provides the knowledge to plan field and cellar work, management wine and grapes market and to invest with more confidence in capital equipment (Diago et al., 2012; Liu et al., 2013). In addition, the result of yield prediction depends on the phenological phase in which it was carried out and also on the different climate and soil conditions of the vineyard plots (Nuske et al., 2011a).

Typically, the yield forecasting is predicted by manual methods, but they are labor intense, expensive, difficult to implement and some are destructive (Nuske et al., 2011a; Nuske et al., 2014a; Di Gennaro et al., 2019). These current methods are also unrepresentative because the estimation is evaluated on a certain percentage of the vineyard and then extended for the whole vineyard (Nuske et al., 2011a; Nuske et al., 2011b; Nuske et al., 2014a).

In the last years, the yield estimation has become one of the most studied topics in viticulture with the aim of finding less invasive, low cost and representative technologies. Moreover, there has been an increase of innovative technologies in agriculture and in the next years these technologies will reach an exponential increase but even higher performance solutions and reduced costs (Diago et al., 2012; Matese and Di Gennaro, 2015). For example, VINBOT robot is a new ground platform that can estimate yield through image analysis methodology (Matese and Di Gennaro, 2015: Lopes et al., 2017; Victorino et al., 2020).

1.1. The aims of the work

The objective of this work is to study a non-destructive, cheap and timesaving technique to estimate yield in order to improve crop-forecasting. Images of the grapevine variety Syrah taken from laboratory and field during the year 2019 by the ISA research team, were analyzed in this thesis.

The first step of thesis work was to collect data with the Vinbot and to develop models to estimate the non-visible berries during the period between the berry pea-size and the harvest stages, in order to obtain the yield estimation. The second step was to estimate yield and to compare it against the actual one.

2. LITERATURE REVIEW

2.1. Precision Viticulture

Vineyards are characterized by a high heterogeneity due to different factors, therefore each parcel has different crop, soil and seasonal weather characteristics that lead to different vine physiological response (Matese and Di Gennaro, 2015; Searcy, 2008). The precision viticulture (PV) is defined as a technique to manage and to monitor of spatial variations in any physical biological and chemical variables that means management differentiation of each parcel of the vineyard in order to fulfil the real needs (Hall, 2002; Matese and Di Gennaro, 2015). The main aim of precision viticulture is minimizing production costs and in the meantime improve crop quality while ensuring the preservation of the environment (Fernandez et al., 2013). Therefore, to achieve this goal, the PV deals with observation and collection data of each vineyard plot in order to apply the correct amount of production inputs (fertilizer, pesticides, seed etc.) and reduce input costs (Searcy, 2008).

2.1.1. The basis of Precision Viticulture

The main objective of the monitoring process is to obtain the maximum amount of georeferenced information in the vineyard. (Fernandez et al., 2013; Matese and Di Gennaro, 2015).

Geolocation is the process that determines the relationship between spatial information and its geographical position. In this way, it is possible knowing the different spatial data detected in the vineyard. Geolocated data are obtained thanks to technologies such as Global Positioning System (GPS), Geographic information Systems (GIS) that are the basis of precision viticulture (Searcy, 2008; Matese and Di Gennaro 2015).

Global Position System is a space based navigation system that calculates its position on the earth through data received by four or more satellites and thanks to a network of fixed ground based reference stations that improve the signal accuracy. The GPS technology is used for tasks that require high precision, such as crop mapping, soil sampling, distribution of fertilizers and pesticides, automatically driven machines and robots. The GPS can be used in combination with Geographical Information System, which is a software able to process and map spatial data in order to help viticulturists to make management decisions (Hall et al., 2002; Matese and Di Gennaro, 2015).

2.1.2. Sensors

In precision viticulture, a wide range of sensors is available to monitor different parameters that characterize the plant features, environment and they are employed in precision viticulture for remote and proximal monitoring of geolocated data (Matese and Di Gennaro, 2015).

Sensors are non-destructive methods that can be used to improve crop management, phenology monitoring, yield monitoring, canopy geometric characterization etc (Genè-Mola et al., 2020). Especially optical sensors can work at different wavelengths, in various domains of the electromagnetic spectrum. The most luminous spectrum regions investigated are:

• Ultraviolet (UV) from 0,01 to 0.40 μm

• Visible (VIS) wavelength in the range from 0.40 to 0.75 μm;

• Near infrared (NIR) from 0.75 to 3 μm;

• Medium infrared (MIR) from 3 to 8 μm;

• Thermal infrared (FIR) from 8 μm to 0.1 cm;

• Microwave (MW) from 0.1 cm to 100 cm. (Brancadoro and Carvanelli, 2010).

These sensors detect and record the light emitted from the surface or ground targets, the amount of light reflected by them is specific for each kind of targets and correspond to the spectral signature. The latter can be represented on XY graph, where on the ordinate there is the reflectance value and, on the abscissa, the spectrum wavelength (Matese and Di Gennaro, 2015). The most common sensors used in precision viticulture are thermal, multispectral, hyperspectral and RGB sensors, all of them supply 2D information. The thermal sensor is used to measure the temperature of the leaf to understand the water stress of the vine. Multispectral and hyperspectral sensors detect the health, nutritional status, and vigor of the vines, but the first one is characterized by a reduced range and less resolution than the hyperspectral sensor. Moreover, recent studies lead to the introduction of 3D sensors. The acquisition of 3D information occurs from depth cameras, structure from-motion approaches, stereo vision and light detection and ranging (multi-beam LIDAR) sensors. LIDAR sensor is able to do a georeferenced 3D reconstruction of each single plant and make spatial variability maps of the volumetric size of the canopy, directly linked with the leaf area index (LAI). These sensors are used to estimate parameters such as crop growth, height, shape and leaf area but also the applications of pesticide treatments, irrigation, pruning and crop training. LIDAR is less used for yield estimation as it is more expensive than the other sensors (Matese and Di Gennaro, 2015; Genè-Mola et al., 2020).

2.1.3. Remote sensing

Remote sensing is a process that involves observing or measuring at distance the characteristics of a particular target, which images can be obtained by satellites, aircraft and unmanned aerial vehicles (UAVs). About satellites their used has great potential but the spatial resolutions are not sufficient for precision viticulture due to the narrow vine spacing, other limitations are linked to the temporal resolution and cloud cover that can occur at the time the satellite passes. Aircrafts monitor the ground with wide flight range and high payload in terms of weight and dimensions; in this way, they are able to manage a large number of sensors. Aircrafts provide higher ground resolution as compared to satellites, depending on the flying altitude. It is economically viable only on areas of more 10 ha because it has reduced flexibility of the time acquisition, due to the rigid schedule of flight planning and high operational costs (Matese and Di Gennaro, 2015). UAVs, sometimes wrongly called “drones”, are fixed or rotary platforms that are able to fly autonomously or can be controlled at visual range by a pilot on the ground. In the first case the UAV is characterized by a complex system of flight control sensors (gyros, magnetic compass, GPS, pressure sensor and triaxial accelerometers) controlled by a microprocessor. These sensors allow performing a wide range of monitoring operations; in fact, UAVs associated with them have a high spatial ground resolution, possibility of highly flexible and timely monitoring, due to reduce planning time. These technology is ideal in vineyard of small size (1-10 ha) especially in areas with a higher heterogeneity. However, UAV platforms have an important limitation in term of payload weight and operating times (Turner et al., 2011; Matese and Di Gennaro, 2015).

2.1.4. Proximal sensing

Proximal sensing technology is characterized by detection of the target features done closely to the using sensors on the ground (fixed or mobile). In this case, sensors can be placed on vehicles like robots, tractors or quad and they work similarly to satellite and airborne sensors (Rosell et al., 2009). An example of this technology is the wireless sensor network (WSN), used to monitor important variables of the grape production, processing the data and transmitting the information to the users. WSN consisting in a network of peripheral nodes characterized by: a sensor board equipped with sensors that detect the information and a wireless module that transmit data from the nodes to a base station. In the latter data are stored and accessible to the end user, while the nodes of sensors are positioned in representative areas of the vineyard (Matese and Di Gennaro, 2015). Another example is monitoring soil variability by measuring the electrical conductivity by mobile platforms equipped with

soil electromagnetic sensors and GPS for continuous measures. The soil electrical conductivity is related to texture and depth, water retention capacity, organic matter content and salinity. Instead, there are many systems to monitor vineyards through the high resolution screening of the canopy side across the row (crop sensors) coupled with GPS. Regarding crop sensors, some examples are: GrapeSense collecting information on the height and the texture of the vines along the row; GreenSeeker and Cropcircle are multispectral sensors that obtain information for vegetation indices calculation. Finally, ultrasonic sensors can allow non-destructive yield monitoring that can be integrated in mechanical harvesters in order to obtain a vineyard productivity. While optical sensors can be used to monitor grape quality such as Spectron which is a portable spectrophotometer for grape maturation monitoring and Multiplex, a portable optical sensor that can quantify the grape polyphenols and chlorophyll content using fluorescence. (Matese and Di Gennaro, 2015; Ferrandino et al., 2017).

2.1.5. Robotic platforms

Use of robots in viticulture is in development and nowadays robotics is still at a prototype stage. In the last years there has been an increase of innovative technologies in agriculture and in the next years, it will reach an exponential increase with higher performance solutions and reduced costs. Following are different examples of robots projects (Matese and Di Gennaro, 2015).

VineRobot project, coordinated by Televitis Research Group at the University of La Rioja, monitors different features such as yield, vigor, water stress and the quality of the grapes and this robot represent a tool to be used as a decision support to the grower to improve the management of the vineyard. The VineRobot is equipped with several sensors like fluorescence, multispectral, RGB for machine vision, thermal infrared, and GPS (Matese and Di Gennaro, 2015; VineRobot, 2020).

The VINBOT project coordinated by the Spanish Robotnick Automation Company, has a robotic platform with open-source software. This robot allowed a 3D reconstruction of the canopy with sensors and it allowed to determine the vine vigor with multispectral cameras and to obtain important information such as the productivity estimation (Matese and Di Gennaro, 2015; VINBOT, 2020)

The Wall-Ye robot is a product developed for vineyard monitoring. This robot can acquire data on each vine and produce a detailed vineyard map and it can carry out precision pruning respecting the architecture of each vine. It can be monitor by an application for the iPad (Matese and Di Gennaro, 2015; Wall-YE, 2020).

The VineGuard robot proposed by Gurion University in Israel is a prototype for foliar applications. This robot has a set of sensors to move, a robotic arm used for grape harvesting and a artificial intelligence to guide the robot in a series of operation such as localization, assessment of the maturation state, selection and detachment of the grapes from the vine (Matese and Di Gennaro, 2015; VineGuard, 2020).

The Vitirover project is produced by Xavier Davis Beaulieu, this robot can cut the grass up to a distance of 2-3 cm from the base of the vine in full respect of the plant. The power system is completely self-sufficient thanks to a solar panel. The Vitirover has a GPS and it can work independently but can also be controlled by computer or smartphone applications for iPhone, BlackBerry and Android (Matese and Di Gennaro, 2015; Vitirover, 2020). Finally, the American company Vision Robotics Corporation has produced a prototype able to carry out precision pruning thanks to optical sensors that perform a 3D reconstruction of the vine structure (Matese and Di Gennaro, 2015; Vision Robotics, 2020).

2.2. Yield forecasting

The yield estimation is an important tool for taking decisions relating to crop load adjustment and yield management in order to optimize plant growth and to improve fruit quality, it also outstands for its economical relevance (Nuske et al., 2011b; Aquino et al., 2018bblomgernhiggin; Di Gennaro et al., 2019;). Therefore, these forecasts are necessary for growers as it predicts the amount of grapes that will be harvested in the year in question (Sabbatini et al., 2012). In fact, the most common form to represent the yield of a vineyard is the amount of grapes and it is influenced by different variables such as vine health, weather conditions, site capability and cropping history. Moreover, the crop load for the same site can vary from year to year due to business and viticultural factors such as soil conditions, diseases, pests, climate and variation in vineyard management practices. (Whalley and Shanmuganathan, 2013; Komm and Moyer, 2015). Therefore, the grapevine yield estimation is subject to a high spatial variability leading to a variability in quality resulting in a greater difference in grape prices (Hall et al., 2002). The method to estimate yield is based on the count of yield components such as number of vines/ha, number of nodes/vine, number of shoots/node, clusters/shoot, flowers/cluster, berries/cluster and berry weight (Martin et al., 2003). The current manual methods are labor intensive, destructive, inaccurate, expensive and spatially sparse. Indeed, the sample size is often too small in comparison to the spatial variability in a vineyard, therefore the yield estimations will be not very accurate (Nuske et al., 2011a). Typical yield forecast is obtained through: knowledge of historical data (e.g. the rainfall, airborne pollen,

temperature, crop yields in 15-20 years) or manually measurements taken in the vineyard. The classical yield estimation methods consist of manual collection and weighting of the crop of limited plant sample previous to harvest, but these yield data maybe not representative. In alternative, yield forecast can be also obtained multiplying the total number of berries and the berry weight (Liu et al., 2013; Whalley and Shanmuganathan, 2013; Acquino et al., 2018). Nevertheless, in the last years the image analysis represents an inexpensive, non-destructive way of capturing precise information about the vineyard in a single crop growth cycle, while traditional methods take into account historical data. Therefore, non-invasive imaging-based methods are used to make possible the efficient and continuous capture of detailed information from plants during their life (Liu et al., 2013; Whalley and Shanmuganathan, 2013).

2.2.1. Manual methods

Manual methods to estimate yield is based on the count of yield components, listed in the previous paragraph. The first step is to determine the number of vines to be considered according to the size of the vineyard. Yield components can be forecasted between the budburst and harvest period and after obtaining the results, they will be extended to the whole vineyard. Therefore, the yield estimation can be inaccurate, since the elements are too small, compared to the space variability of the field (Martin et al., 2003; Nuske et al., 2011b). In fact, for this reason, a more intensive sampling is carried out in order to obtain higher reliability of yield estimation. The spatial variability is correlated especially from the environment that individual plants such as meso-climate, edaphic factors etc., this point like annual variability entails problems in the management of the production (Dunn et al., 2014). Moreover, the yield component bunches per vine is the major contributor of yield variation (60%-80%) for Cabernet Sauvignon, Chardonnay and Shiraz (Dunn et al., 2014).

Usually yield forecasts are conducted in the period from budbreak to just before harvest, but a very early yield forecast can be obtained during dormancy (before budbreak), estimating node fertility. Yield can be forecast through equation 1, considering bud fruitfulness index (IF) that is obtained as inflorescences per bust node (Clingeleffer et al., 2001; Dunn et al., 2014):

*Yield (t/ha) = (IF season/ IF previous seasons) * historical average yield (t/ha)* *Equation 1*

In Clingeleffer et al., (2001) study it was shown how counting total nodes, shoots, fruitful shoots, bunches per vine and the percentage of bud burst, by the Merbein bunch count method, yield components that allow to obtain a yield prediction. These predictions are carried out between budburst and flowering like the assessment of flowers number per clusters since before that period

clusters are not visible (Martin et al., 2003). Since the manual flower number counting is a time-consuming process, there is another efficient method to count them, which examining a good relationship between inflorescence length, dry weight and flower number. These last techniques allow an early berry number prediction, but it is affected from the fruit-set conditions (Dunn et al., 2014).

The early forecasts are imprecise, because they are subject to many factors as the flowers number estimation is affected by vigor, number of nodes, cluster order, temperature, irradiance, biotic and abiotic stress. However, the most promising early yield predictor is the number of primary branches. In fact, in Clingeleffer et al., (2001) and in Dunn and Martin, (2007) studies, showed that the number of primary branches per inflorescence had a high influence on the total flowers number per inflorescence and consequently on the bunch weight, in addition, in both studies this relationship was stable season to season.

The number of berries depends on the total number of flowers but especially on the amount of these that set successfully and are maintained through the harvest. (Dunn and Martin, 2007). These can be forecasted at any time until harvest, but usually there are many berries lost after flowering, so the better estimation is assessed after fruit-set and before harvest. Therefore, it is possible to calculate the yield prediction through the formula (Eq. 2) from Clingeleffer et al., (2001), knowing the number of berries per bunch, the number of bunches per vine, the total number of vines and the berry weight:

*Yield (g) = n. of vines * #bunches/vine * #berries/ bunch * berry weight (g) * harvest efficiency Equation 2*

The equation 2 estimates the bunches/vine from bunch counts, berries per bunch through sampling bunches, predict average berry weight (historical data) and lastly harvest efficiency. The latter is calculated as the ratio between the amount of grapes arrived in the cellar and in the patch at harvest, it takes values from 0.85 (inefficient machine harvesting with transport losses) to 1 (hand harvesting very close to the winery) (Dunn et al., 2014). Clingeleffer et al., (2001) showed a high margin of error in the yield estimation (with equation 2) might be caused by the difference in the number of berries per bunch between the post-fruit set and pre-harvest. This error may be partially attributed to the multiplication of the berry weight (historical data), this happens because environmental and cultural factors that may influence it are not taken into account in that equation 2.

In Dunn et al., (2014) yield estimation based on berry count carried out after fruit set, allows an error of around 15%-20%. As said above, yield can be estimated at any time during the growing cycle of the vine. However, to obtain more accuracy, predictions can be done near to harvest, for this reason veraison is a good time to predict it. Yield forecasting can be calculated using historical data and berry growth factor as in the equation 3 and 4 (Clingeleffer et al., 2001).

*Bunch weight $_{harvest}$ (g) = Bunch weight (g) * berry growth factor* *Equation 3*

Berry growth factor= cluster weight at harvest ($_{historical\ data}$) / cluster weight $_{(veraison)}$ *Equation 4*

Close to harvest, usually a week or few days before it, it is a good time to estimate yield because there is very little change in the crop weight. Moreover, if predicted yield is carried out in accurate way, the value will be close to the actual yield. Clingeleffer et al., (2001) proposed the equation 5 to estimate yield from historical data (average yield):

*Yield (t) = (average yield (kg) / vine * total number of vines / vineyard) / 1000 Equation 5*

2.2.2. Aeropalynological method

Aeropalynological forecast model (APFM) is an instrument that allows the yield estimation during flowering stage, measuring the pollen concentration in air. It is a valuable tool as it takes into account factors such as preflowering conditions, plant vigor and health that influence the crop production (Cunha et al., 2003). According to Cunha et al., (2003) study the pollen was captured by using Cour trap that was placed in an upright according to the wind direction during pollen season for a period of 3-4 days. In this method the pollen grains captured by hydrophilic vertical gauze filters with an area of 400 m^2, are expressed in number of pollen grains/m^3. It is possible to make an equation or model relates the amount of pollen with the amount of wine production. APFM shows a good regional crop estimation, but some disadvantages of this estimation model are the complex laboratory process and it does not allow separating pollen by variety, region or producer (Cristofolini and Gottardini, 2000; Cunha et al., 2003).

2.2.3. Trellis tension method

In Blom and Tarara, (2009) study, a dynamic method of yield estimation against to traditional static methods is analyzed the trellis tension method (TTM). This system is based on the tension changes

of the wire, which supports the main trellis. The yield forecast is obtained from the following equation 6:

$$Y_{t,c} = (Y_a / T_{t,a}) * T_{t,c} \qquad \textit{Equation 6}$$

Where $Y_{t,c}$ is the yield predicted at any time (t) of the current year, Y_a is the yield from an antecedent year, $T_{t,a}$ is the trellis wire tension at the time t from the antecedent year, $T_{t,c}$ is the wire tension at time t of the current year. It has been demonstrated that the margin of error of the use of this model is equal to or slightly lower than traditional methods. Moreover, the authors explain that in order to improve the estimation of the yield through TTM, it is necessary to have a greater number of historical data on which to base the forecast.

2.2.4. Agrometeorological models

Agrometeorological models are obtained from multiple regression between climatic variables measured during relevant phenological phases and yield. Therefore, it allows a better understanding of the relationships between climate and yield. Crop estimation can be obtained through descriptive methods, linear regression or yield simulations. This model analysis the behaviour of the crop based on the main climatic variables such as temperature, rainfall, soil moisture etc., to which it is subjected. This method is very variable and not easy to extrapolate, for this reason it is less used in yield estimation (Sivakumar et al., 2000).

2.2.5. Image analysis

As explained above, manual methods to estimate yield are laborious, subjective and time consuming (Tardaguila et al., 2013). In this regard, recently, it has been developed indirect method to have a rapid and accurate yield forecasting based on computing and assessing the image analysis acquired with video and digital imaging. The technique allows the automated analysis of grapevines videos and images taken manually or from sensors positioned on vehicles such as tractors, quad, remote controlled and robotic vehicles previous mentioned (Fuentes et al., 2014).

In Tardaguila et al., (2013) study, it is being confirmed that image analysis represents a simple and computationally cheap method, without the need of contact to assess canopy features and yield estimation, indeed this study shows the strong relationship between the yield and the data obtained using computer vision. Therefore, this method is an important tool that offers the advantage to collect data like images or videos that will be studied by image analysis system able to

acknowledge objects in images using algorithms and different methodologies (Fuentes et al., 2008; Tardaguila et al., 2013; Victorino et al., 2020). Therefore, image analysis as manual methods are used to detect yield components such as shoots, flowers, bunches, berries and bunch traits in different phonological stages (Victorino et al., 2020). However, image analysis are used more to determine leaf area rather that the yield since the visibility of yield components are limited and less exhibited to the sensor. Visibility of yield components is affected to different factors such as shape, size, color (bunches) and quantity of them, but also canopy development, especially during the ripening period and harvest in non-defoliated situation. These factors are in turn influenced by the characteristics of the variety such as bunch compactness, vigor, leaves shape and length of the internodes. (Diago et al., 2012; Fernandez et al., 2013; Victorino et al., 2020).

2.2.5.1. RGB and HSV color spaces

The most known and used image-acquisition method is the application of colour-based to detect grapes in images. It is an easy, cheap and non-destructive technique based on the separation in the RGB and HSV color spaces; it is necessary only a commercial RGB (Red, Green and Blue) camera (Diago et al., 2012; Fernandez et al., 2013; Liu et al., 2013). This method requires a 2D sensor, which gives 2D information, and it is useful for yield mapping and monitoring (Genè-Mola et al., 2020). After the acquiring of the RGB image, the second step is to transform it to L*a*b* color space known as CIELAB color space (*Fig. 1)* (Fernandez et al., 2013).

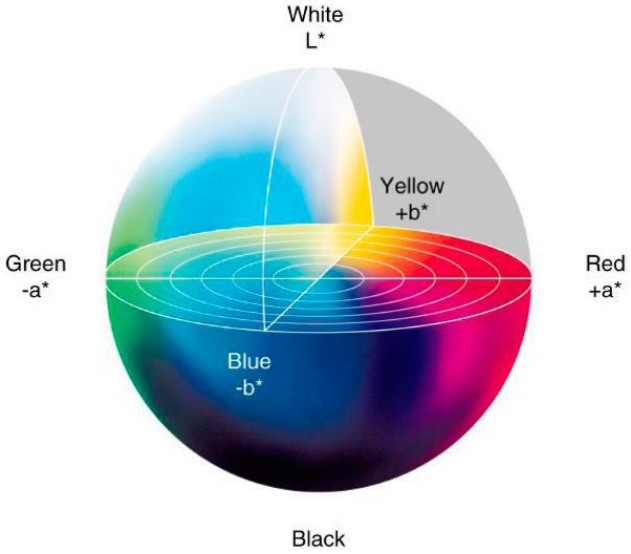

Figure 1. CIElab colour space (Cortez et al., 2017).

The latter is an international standard for color measurement developed by the *Commission International d' Eclairage* (CIE) in 1976 (Diago et al., 2014). Coming back on the three coordinates they are: "L*", which represents the luminosity layer, "a*" the chromaticity-layer indicates where color falls between red-green axis and "b*" indicates where the color falls between blue-yellow axis. These represent the description of the color that is hue, saturation and brightness (HSB), the first one tells if the color is red-green, blue-yellow, the saturation tells the level of the color intensity and the brightness tells the color light intensity (Cotton, 1996; Tkalčič and Tasič, 2003). To understand a scene or the characteristics of the images, it is used the Computer Vision. The latter is an Artificial Intelligence that includes an illumination system, a charge-coupled device (CCD) that converts the images obtained from the camera into a digitized one, and a computer with an adapt software for image processing and interpretation of the results. The illumination system is an important tool because it helps to identify the objects and the color calculation process needs a light standardization (Rodriguez-Pulido et al, 2012). First, to carry out the image processing there is need to determine a region of interest (ROI) to analyze (Diago et al., 2019).

2.2.5.2. Image segmentation

The next step of image analysis is the image segmentation. It is a process that deals with dividing images into segments. Segments are objects or part of them, constituted in sets of pixels. Image segmentation arranges pixels in greater components to eliminate the need to consider individual pixels as units of observation (Minaee et al., 2019). Segmentation represents the basis for the detection and classification of the images. It is divided in two levels: semantic segmentation and instance segmentation. The first one classifies pixels in classes defined as "bunch", "trunk", "shoot", "leaf", "gap" and "trellis". While instance segmentation identifies each instance of each object. (Diago et al 2019; Minaee et al., 2019).

In the last years image segmentation using deep learning convolutional neural networks (CNNs) that is an improvement of the standard neural network (NN). NN is an algorithm that allows the computer to learn descriptive criteria of the desired image regions just from the image data itself (Rudolph et al., 2019). It is a mathematical model imitate the human brain, in fact connected processors called neurons form it. (Reyes and Sastre, 2014). CNN includes two main phase, the first one is the extraction of features, where in multiple convolution layers alternate to pooling layers

generate more complex class features, in order to reduce the image size in pooling levels. The second one is the classification phase where multiple fully connected layers derive class labels based on the derived image features Fully Convolutional Networks (FCNs) use convolutional layers to process different input sizes, while CNN cannot manage. Convolutional layers classify every pixel to determine the context of the image. In fact from FCN transforms the height and the width of the intermediate layer feature map in the input image size. (Minaee et al., 2019; Rudolph et al., 2019). In the last years, this method was improve in Mask Region-based Convolutional Neural Network (Mask R-CNN). The aim is to differentiate each individual object (object detection) and classified in order to determine its exact location and differentiate it from any other object (even belonging to the same class).The region-based networks extract possible Regions of Interest (ROI) (object detection), then the characteristics of each region will be obtain by using CNN (Zabawa et al., 2020).

There are also other image segmentation techniques commonly used:

- Thresholding: divides an image in a foreground and the background. The images are converted to binary images and a specific threshold value separates pixels in one or two levels (Minaee et al., 2019).
- K-means clustering: an algorithm assigns each pixel to one of the groups (K represents the number of groups) based on the feature similarity. Therefore, does not work on already defined groups but forms them (Minaee et al., 2019).
- Histogram-based image segmentation: uses a histogram to group pixels based on “grey levels”. The background is a defined grey level and it is the biggest entity. Therefore in the histogram, it is represented as the large peak, while the object represents the smaller peak with another grey level (Otsu, 1979; Minaee et al., 2019).

2.2.5.3. Image analysis to detect shoots

An early yield estimation allows to growers to regulate sensibly yield. In Liu et al., (2017) an automatic system was developed to count shoots prior to fruit-set in order to estimate yield. A robust shoot detection framework was used combined with an algorithm. Data were collected in form of videos of shoots, it was taken during day time, therefore there were different adversities to overcame: varying lighting conditions, shadows, change of shoot position in the field of view, reflections, objects in the field of view such as cordon, wire, posts, ecc. To solve these issues, images from videos were divided in sub-windows and processed as object candidates. Given that

illumination conditions changed during the video, it was not possible to apply the common segmentation method that is converting images in a binary one using a threshold value. Therefore it was replaced with a dynamic threshold method proposed by Otsu (1979). Since each time illumination conditions and scenario changed labels are required, it was proposed an unsupervised feature selection based on the correlation of three filters (Kendall et al., 1946; Higgins, 2003; He et al., 2005). In this study particularly good results were obtained accuracy of 86.8% and harmonic average (F1) between Recall (the percentage of actual berries detected by the algorithm) and Precision (the percentage of berries correctly detected) of 0.90 considering that the forecast was done before fruit-set stage.

2.2.5.4. Image analysis to detect flowers

Yield estimation depends mainly on two phenological stages: flowering and fruit-set, as they define the number of berries per bunch. The fruit-set is subjected to varietal and clonal variability and it is affected by physiological, environmental and pathological factors. Therefore, it may be possible to obtain an accurate fruit-set estimation by counting the number of flowers per inflorescence through image analysis. The latter is cheaper, faster and simpler than manually method and the main objective is to improve the quality of forecasting. Three steps characterize this method; the first one is the image pre-processing involving conversion of the image from RGB to CIELAB color space and an initial segmentation separating the flowers from the background. The second step is the flowering counting, where flowers correspond to brighter areas as they present a higher degree of light reflection. The third step is to remove other material than flowers from the brighter area selected. The results have been validated from the software and in addition it has been showed the conjunction between yield estimation through the flowers number and fruit set rate (Diago et al., 2014, Aquino et al., 2015; rn et al., 2017). Rudolph et al., (2019) show another cheap and non-invasive approach to estimate the number of flowers. The method is divided in four steps, the first is image taking with camera; the second is the identification and localization of inflorescences through the image segmentation FCN ideal for small geometry and high density of flowers. Then the flowers were extracted and finally data were evaluated.

2.2.5.5. Image analysis to detect the bunches and berries

As previously explained traditional method to detect bunches and berries are expensive and time consuming, while method based on image analysis are fast, accurate, simple and inexpensive (Diago et al., 2014). Grossetete et al., (2012) show how to detect the number of berries using photos taken with the Smartphone camera during the period between flowering and veraison. Images analysis are obtained using an integrated flash, because berries surface reflects the light and the maximum point of reflection is on the center of them. The image analysis is made thanks to an image processing algorithm is based on the correlation between the Gaussian profile and the neighborhood of each pixel, called correlation map. The white pixels correspond to the reflection areas of each berries, but more specular area can occur on the same berry, therefore the last step deals with solving the issue by morphological dilation. Moreover, several authors, were able to obtain a strong relationship (R^2=0.92) between the real and estimated number of berries by using a polynomial model. (Grossetete et al., 2012). The real value was detected by counting the number of berries manually for each image of the bunch taken with the Smartphone. This procedure was carried out for several years, on different cultivars and in different areas (Grossetete et al., 2012).

Other methods use RGB images but they are distinguished by image processing. In Diago et al., (2012) the images are obtained before and after defoliation and cluster thinning. In addition, a white background was placed behind the canopy in order to avoid confounding effects from background and no artificial illumination is used. This method allowed the images set process, the discrimination of the canopy in seven different parts or classes (grapes, wood, background and four classes of leaf and the increasing of leaf age) and the calculation of their areas (*Fig. 2)* (Diago et al., 2012; Fernandez et al., 2013). Each class is being focused by selecting a set of representative pixels for each part in order to obtain the clustering around them. In Diago et al., (2012) study is shown an accurate estimation of the leaves and the grapes in fact the classifier of the performance for the identification exceeded the 90%. After defining ROI, the image analysis is carried out by a clustering algorithm based on the Mahalanobis distance that deals with identifying the pixels of each class. The Mahalanobis distance measure the similarity between an unknown sample group and a known one. Therefore, the algorithm uses a known sample of values to classify an unknown set of pixels into groups, based on the RGB color values of each pixel. After that, pixel samples for each group are selected manually and some indices are computed by image analysis (Diago et al., 2016; Diago et al., 2019).

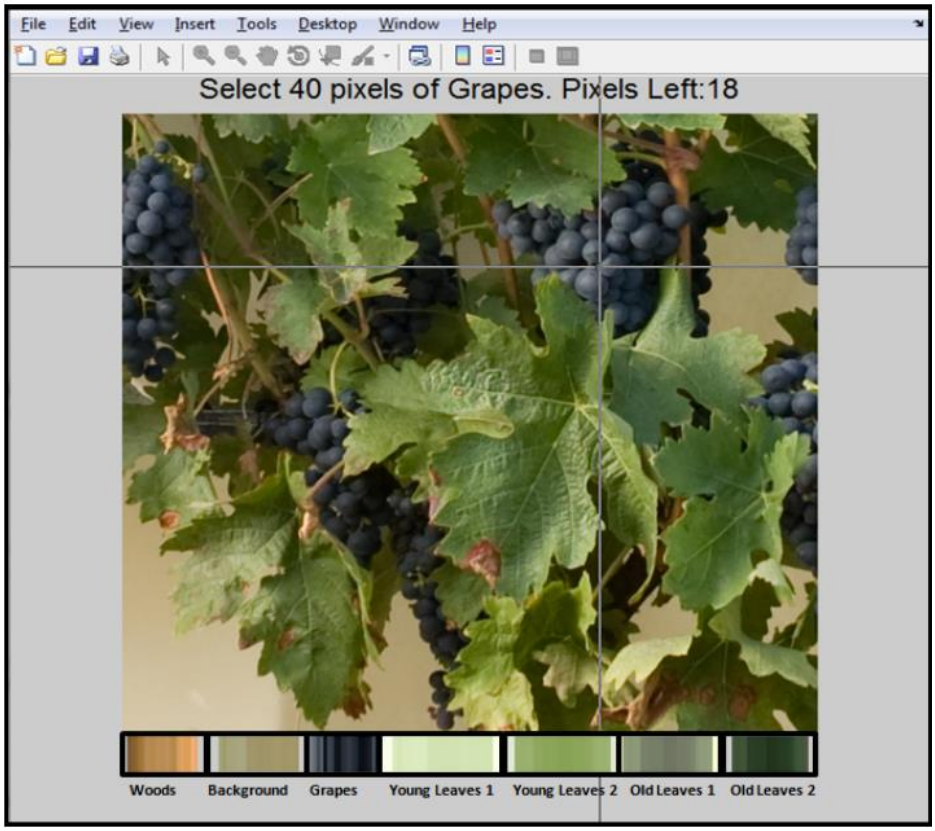

Figure 2. Example of manual selection of reference pixels (Diago et al., 2012).

In Nuske et al., (2011a) study, the RGB camera is mounted on a vehicle and the yield estimation is made before veraison. The algorithm used for image analysis has three steps. The first one is to detect the potential position of the berries with the radial symmetry transformation (Loy and Zelinsky, 2003) that uses the circular shape of berry to detect it. The second step is to identify with deep learning FCN the points of grapes or not-grapes. The last step is to group the nearby berries in clusters. Finally, the authors compared the estimation of berries number with the harvest crop weights to test the yield forecasting accuracy. Further berries were not counted by the algorithm due to occlusion berry-by-berry, yet despite this, the linear regression between berries detected and harvest crop weight showed a R^2=0.74. They demonstrated that is possible to obtain automated yield estimation with an error of less than 9.8 % of the real weight, analyzing the shapes and the texture of the berries (Doutor et al., 2018).

In Nuske et al., (2014b) study was presented an efficiently method to detect and count automatically berries. The work is carried out during the night using camera system mounted on a ground-vehicle and the illumination to optimize for low motion blur. The authors developed an algorithm based on three main visual cues: color, shape and texture. First of all, it was estimated

berries position in the images using a shape transform, after that classify these locations using color and texture descriptions. Moreover, a second camera facing backward from the vehicle is positioned to trace its position in order to avoid a multiple count of a single berry. They were shown a linear relationship between the image berry count and the harvest weight with a R^2 between 0.6 and 0.73.

Aquino et al., (2017) has used a smartphone camera for image acquisition to estimate the number of berries per bunches during the night on five different varieties. After the acquiring of the RGB image, it is transformed it to L*a*b* color space. First, to carry out the image processing there is need to determine a region of interest (ROI) to analyze. After that, the image analyses are developed by MATLAB using the berry-segmentation algorithm. This latter includes two steps, in the first one a set of berries candidate are extracted from the image by means of a morphological filtering, the bright spots produced by the light reflection on the berries surface detected by finding regional maxima illumination. The second step provides for the discard of the candidates that do not corresponded to berries, named false positive. To determine them the authors consider six descriptors and use them to test and compare two different methodology that are Support Vector Machines (SVM) and Neutral Networks (NN). Then, a probability map in form of image is created with the values obtained from NN. After this, the new image is binarized using the threshold automatically provided by Otsu's method (Otsu, 1979). Moreover, the linear correlation between the number of the real berries per cluster and the number of berries per cluster automatically detected, show a R^2=0.75. In Aquino et al., (2018a) the berry-segmentation algorithm was improved in terms of the percentage of berries detected and berry classification, increasing from six to fourteen the number of descriptors to discard false positives. In fact, it was recorded an increase of Recall and Precision, than the values obtained in Aquino et al., (2017). In addition this algorithm tested initially using Matlab, was ported to smartphone through vitisBerry app (*Fig.3*).

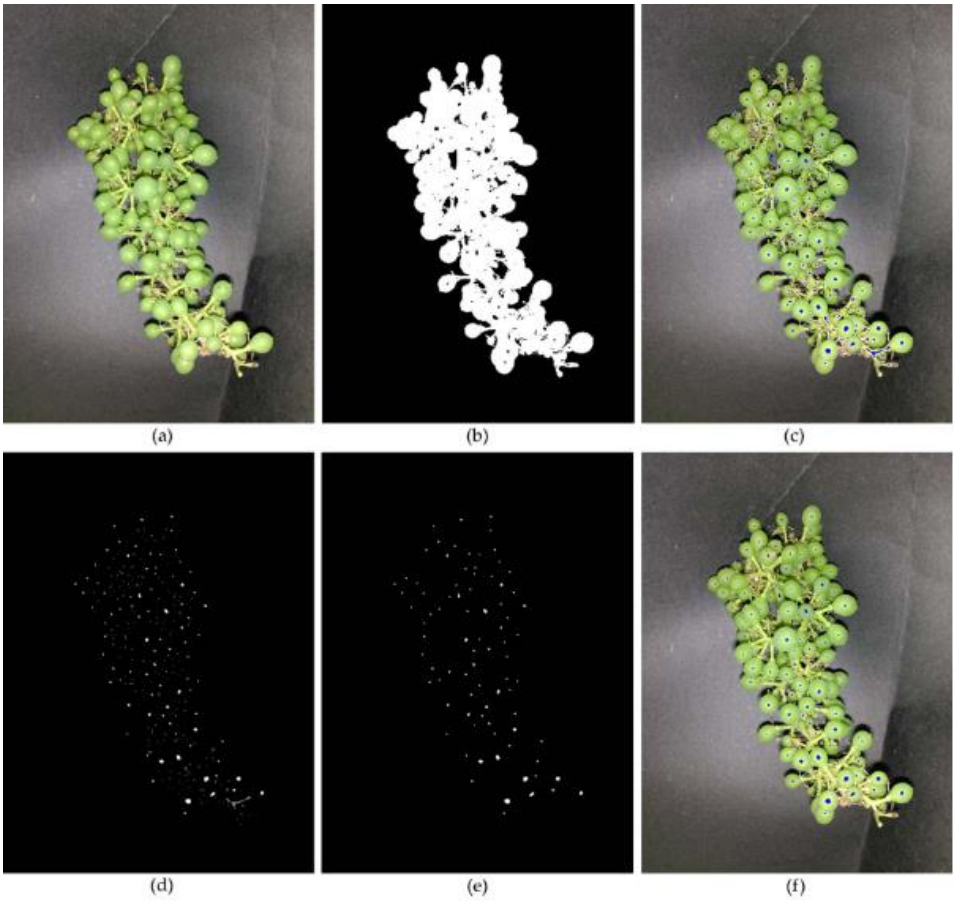

Figure 3. Illustration of the berry-segmentation algorithm on cluster images included in the vitisBerry application: (a) original image; (b) extracted ROI; (c) berry candidates represented in blue colour; (d) image in which each candidate is represented according to its computed probability of being berry (the brighter, the higher probability); (e) binary image illustrating the candidates confirmed as berry; (f) final result showing the found berries (Aquino et al., 2018).

NN method was used also in Behroozi-Khazaei and Maleki, (2017) work that develop an algorithm to segment bunches, obtaining the 99.4% of accuracy.

In Herrero-Huerta et al., (2015) study, 3D models of grapes that were obtained in field were used to estimate yield. This work proposes a non-invasive, accurate yield estimation and low-cost method with the aim to eliminate the subjectivity due to temporal and spatial variability of grape production. The method was a combination between Photogrammery Workbench software developed by the authors, used to reconstruct bunches in 3D model and compute vision. However, the 3D models generate some issues such as having only the visible side of the bunch or having

deal with the occlusion and geometrical complexities of the bunches themselves. The first problem it is solved by the acquisition of the image such as their position, because will affect the final accuracy (in term of prospective ray intersection) and completeness in terms of overlap between image) of the 3D. Finally it was studied the relationship between actual and estimated number of berries obtaining a R^2= 0.80.

In Lopes et al., (2017) work canopy features and yield were estimated comparing the real data with the estimations obtained by the VINBOT. The images were analyzed using image analysis algorithms (ImageJ 1.48V) where the bunch area was extracted, and then it was computed in pixel and converted into actual cm2. Finally, the estimated area of bunches was converted into kilograms. In this study, it was demonstrated an acceptable performance for canopy features estimation but an underestimation of real yield mainly due to bunch occlusions.

In Santos et al., (2020) grapes detection was based on a state-of-art artificial vision system that relies on convolutional neural networks (CNNs), that deals with the classification of the images and three-dimensional associations. CNN can solve several problems found in other methods such as variation in pose, illumination, shape and large inter-class variability, obtaining accurate results. The first step of this technique is named semantic segmentation (a pixel classification to determine fruit), the second step was the fruit localization by bounding boxes. The last step is the instance segmentation that is the identification of berries pixels in the box, thanks to that the occlusion of leaves, trunks, other clusters etc. can be addressed (*Fig.4)*.

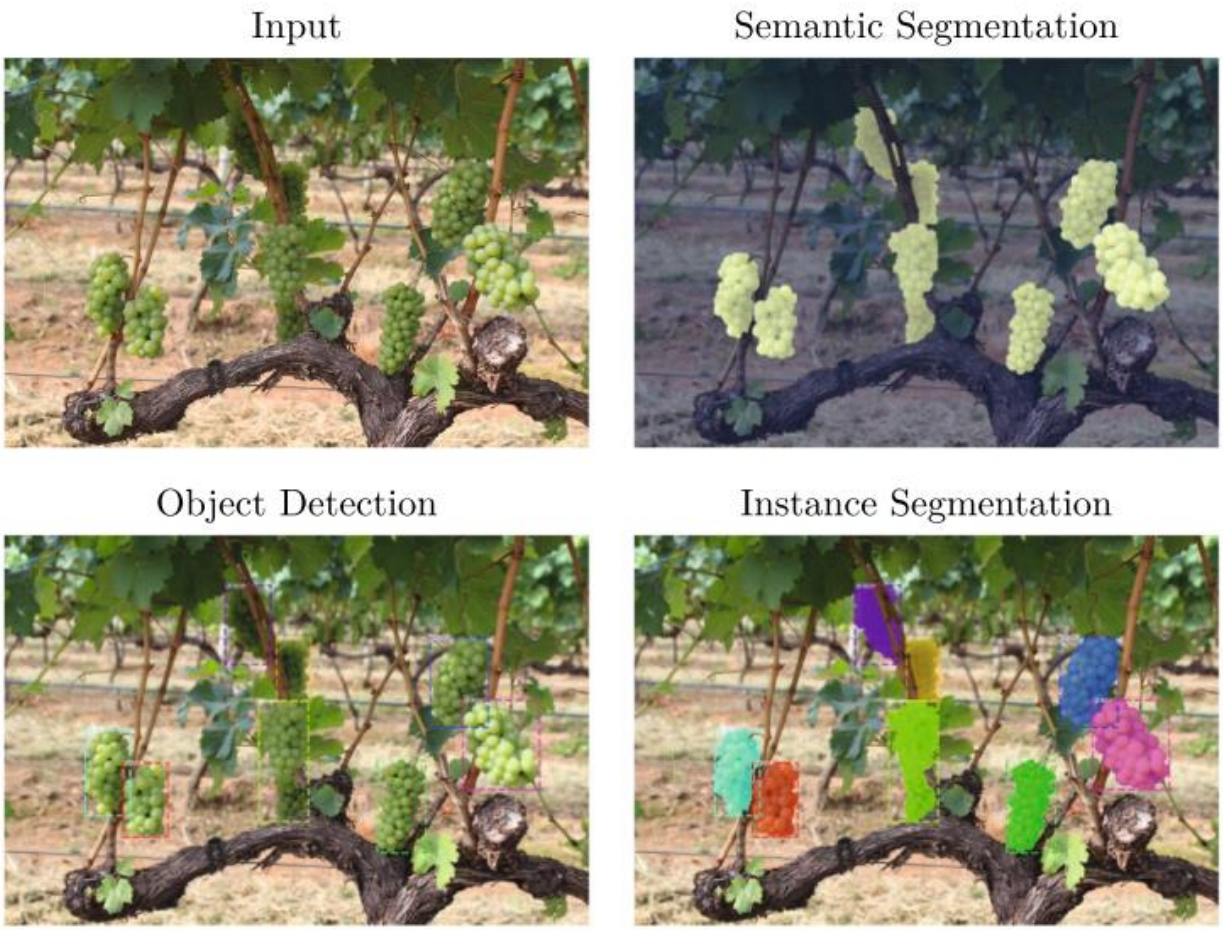

Figure 4. Example of different steps for grapes detection (Santos et al., 2020).

In this study, it was calculated F1, achieving values superior to 0.9, despite the difficulty of berries detection due to shape, size and compactness. Therefore, this method allowed a more accurate assessment of berries number, with the separation of each cluster from other structures in the image that allows a more accurate assessment of fruit size and shape. Moreover, they showed that 3D models produced by structure-from-motion or SLAM Simultaneous Localization And Mapping can be employed to track fruits, avoiding double counts and increasing tolerance to errors in detection.

In Zabawa et al., (2019), Phenoliner, a field platform based on a grapevine harvester was used to acquire images replacing harvest tools with camera to take photos. Single berries were detected in images through an automatic and robust detection pipeline based on the definition of three classification classes “berry”, “edge” and “background” and the application of a neural networks. Every berry was colored with one of four colors and then, an edge was estimated with a determined size. This kind of classification helped the differentiation between single berries in the cluster. A

connected component algorithm determined the number of berries. In addition it allowed not only the counting and identification of the position of berries, but also the investigation of their size. Finally, berries were detected with an accuracy of 94% in the Vertical Shoot Position (VSP) system and in a Semi Minimal Pruned Hedge (SMPH) with 85.6%. This is caused by a major covered of grapes by canopy in SMPH, while in VSP, grapes are positioned on the bottom of the canopy and they are not much occluded. In Zabawa *et al*. 2020 study, the results obtained with the approach mentioned in Zabawa et al., (2019) was compared with two different images segmentation methods, the Mask-RCNN and U-Net (popular architecture of FCNs) (Rudolph et al., 2019). The new method, achieved a major accuracy against the other two. However, the correlation between detected and actual berries was very high and better than in Zabawa et al., (2019), but the tendency was to underestimate the berries number, due to the bunch compactness. Furthermore, unlike the other methods, approach can be inferred in minutes. The advantage of this new approach is the potential extraction of additional phenotypic traits like the berry size.

Coviello et al., (2020) developed a smartphone application named Grape Berries Counting Net (GBCNet) able to estimate yield. Images taken with a regular smartphone camera were processed by app obtaining a density map and after the application of deep learning algorithms; the number of berries was estimated. In this study, data are collected directly in field without the need of special cautions or contrast tools. The average error for the berry detecting was of 5%, however this value could drop through the analysis of over more three pictures from the same parcel.

In Liu et al., (2020b) study, it was presented an algorithm able to count berries and to estimate the 3D reconstruction in three main steps. Berry counting was based on a single image of red or green bunches. The original photo was cropped and segmented from the background. The berries on the edge are fitted following the curvature and then the remaining berries were placed inside of the outline (*Fig.* 5)

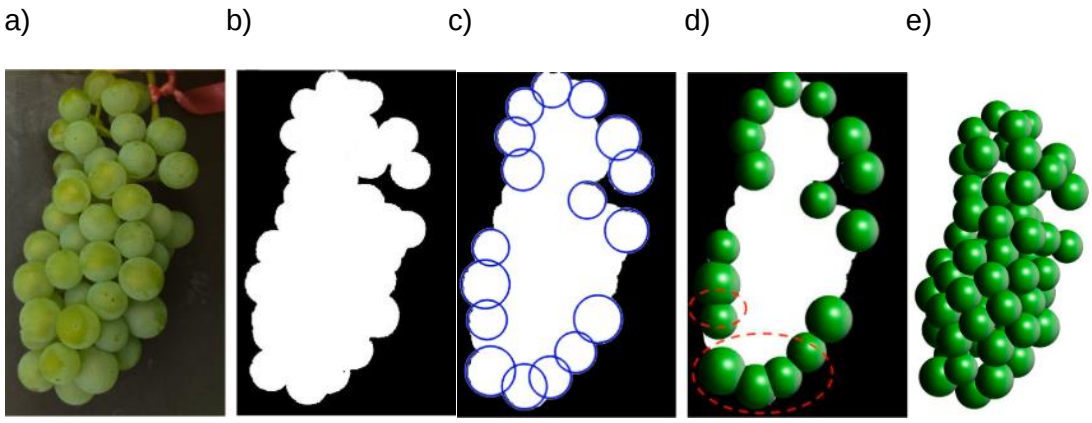

Figure 5. Representation of a Chardonnay bunch. a) The original photo. b) it was segmented from the background. c)-d) From this segmentation, berries were fitted following the outline curvature. e) Remaining berries were placed inside the hull formed from the segmented outline (Liu et al., 2020b).

Berries were counted through a robust calibration-free algorithm and final berry number was obtained through the estimated berries number and the sparsity factor. 3D model did not take into account the empty space inside the bunch, thus obtaining an overestimation of the berries. To solve this issue, the sparsity factor was introduced to process both red and green grapes based on the visible proportion of berries in the cluster area.

The accuracy of the approach was 89% if directly compared with the berries number of the bunch. Instead, when more images were considered the accuracy was over 99%. Liu et al., (2020a) developed an application for smartphone named 3Dbunches based on the algorithm mentioned in the previous work (Liu et al., 2020b). This app recorded an accuracy of 91%. Moreover, the percentage of error for yield estimation was encouraging for the berry-counting algorithm.

2.2.5.6. Image analysis to detect bunch traits

Yield components, to estimate yield include not only shoots, flowers, bunch and berries (paragraphs), but also bunch traits such as bunch area, volume ecc. (Font et al., 2015; Herrero-Huerta et al., 2015). In Font et al., (2015) and in Hackings et al., (2019) bunch area was obtained as the number of pixels in the segmentation image and volume was estimated from it, while in Herrero-Huerta et al., (2015) used the reconstruction in 3D of bunches to detect volume. In these study bunch area/volume were converted in bunch weight obtained from their relationship (Lopes

et al., 2016). In fact, these bunch traits can be used as proxies to estimate bunch weight, subsequently used for yield forecast (Victorino et al., 2020). This is possible due to the fact that exists a high correlation between bunch area/volume and bunch weight, therefore (Font et al., 2015; Hacking et al., 2019).

3. MATERIALS AND METHODS

Due to the COVID-19 pandemic, it was not possible to carry out by myself the work in the vineyard and in laboratory. To solve this problem, Images and data collected during 2019 growing season by the ISA research team were used in this thesis. The images were sent to us and our main work consisted in counting the number of visible berries on each image.

3.1. Site characterization

The images and part of data, analyzed in this work, were obtained during the year 2019 at the educational vineyards of the Instituto Superior de Agronomia (ISA), in Lisbon with the coordinates 38°70'92.86''N, 9°18'72.42''W and 62 m above sea level (*Fig.6*).

Figure 6. Map from Google Earth of ISA Vineyard where cv Syrah is located.

The grapevines of the variety Syrah, are trained to a vertical shoot positioning trellis with two pairs of movable wires and spur-pruned on a bilateral Royal Cordon system and are spaced 1.2 m within and 2.5 m between north-south oriented rows. The field has a slop of 11%. The soil is a clay loam with 1.6% organic matter and a pH of 7.6. Cv Syrah was planted on 1998 and grafted onto the rootstock 140 Ruggeri (*Vitis berlandieri* x *Vitis rupestris*) (Samà, 2019), it is a rootstock with high vigour and more resistant to dryness and at the presence of limestone (Cosmo et al., 1958).

3.2. Climatic characteristics

The climate in Lisbon is characterized by moderate rainfall in winter and deficit in summer (Kottek et al., 2006). Average annual precipitation, from 1971 to 2000, was 725.8 mm, with minimum values recorded during summer months and maximum values obtained during winter months. Average annual temperature values were 16.4°C, with an average minimum value of 11.8 °C obtained in winter and an average maximum of 21°C recorded in summer (IPMA, 2019). In the *Figure 7* it is possible to note that the rainfall during the season 2019, were lower than the average of the last 30 years, except for the April month that it was the wettest one.

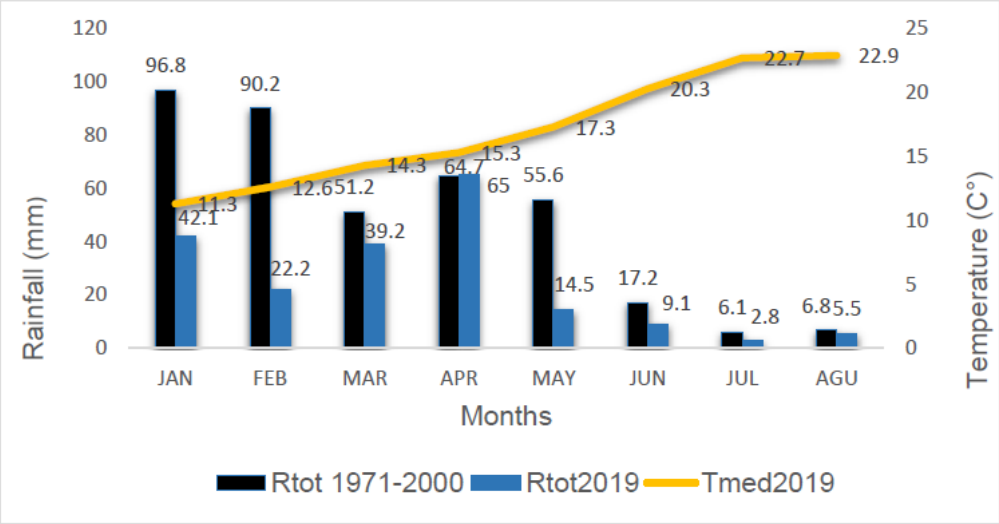

Figure 7. Rainfall and average temperature during 2019 growing season (IPMA, 2019).

3.3. Studied variety

Syrah is one of the varieties called “international” because they have been exported from France and cultivated all over the world. In terms of yield, it shows a medium high productivity and a high vigor. The grape Syrah has a medium compact cluster, medium sized, cylindrical shape and with the number of wings ranging from zero to one (*Fig.8*). Regarding the berries, they have a medium size, ovoidal shape with a very pruinose skin and blue-black color (Quattrocalici, 2020). About diseases, cv. Syrah has a normal resistance to the common parasites of the vine. It seems to have an excellent resistance to black rot (Breviglieri and Casini, 1962).

Figure 8. Bunch of Syrah imaged at the lab.

3.4. VINBOT

Vinbot is an autonomous cloud-computing vineyard robot and it is part of an EU project. The main objective of this new platform is to optimize the yield forecasting by means of cloud computing applications that take in count the spatial variability of the vineyard plots. Vinbot can estimate the amount of leaves, grapes and other phyto-data, navigating through the vineyards capturing geolocated 2D and 3D images thanks to different kind of sensors. In addition it is able to climb slopes up to 45°. It is powered by an electric battery and can work 8hrs per day. This robot can generate online yield and vigor maps to help winegrowers optimize management strategies.

The Vinbot consist of (*Fig. 9*):

- A robotic platform: mobile, durable with open-source software.
- Color camera: RGBD Kinect to take images of the vine.
- 3D range finders to obtain the shape of the canopy and to navigate the field.
- A Normalized Difference Vegatation Index (NDVI) sensor to compute the vigor of the plants.
- A small computer for basic computational functions and connected to a communication module.
- A cloud-based web application to process images or create 3D maps.

- User friendly Human Machine Interface (HMI) to define navigation and data acquisition missions.

(Reyes and Sastre, 2014; Lopes et al., 2017; VINBOT, 2020).

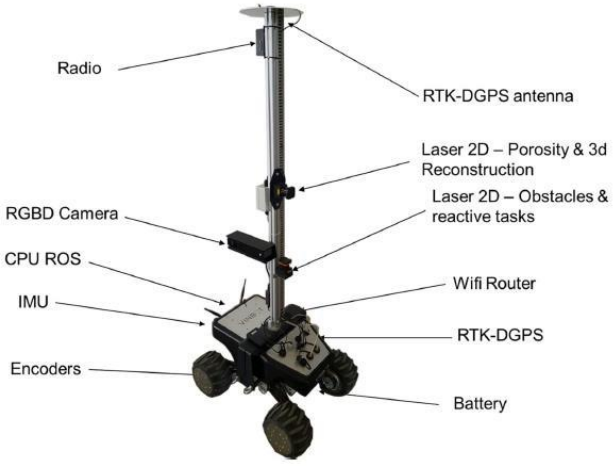

Figure 9. Vinbot view (Guzmán et al. 2016).

3.5. Experimental design

In 2019, two rows (14-15) of 25 meters length were selected in the vineyard plot for data collection. Then, within these canopy segments named Smart Points (SPs); SP1 was at the beginning of the row number 14 and SP2 at the end of the row 15, in order to encompass as much as possible, the variability present in the vineyard. The red rectangles in the Figure 4 show the 10 meters segment which were photographed by the Vinbot at three important phonological stage: pea-size, veraison and maturation. These segments were labelled by a measuring tape attached to the base of each vine in order to obtain a better identification of the images as well as a static scale. Adjacent to these rows, other segments were selected at each of the analyzed phenological stage, in particular 5 meters at pea size (yellow line), veraison (green line) and maturation (blue line) (*Fig.10*). These segments were photographed manually using a commercial RGB camera at different levels of defoliation: low, medium and full (Samà, 2019), as explained in the 3.5.2 chapter.

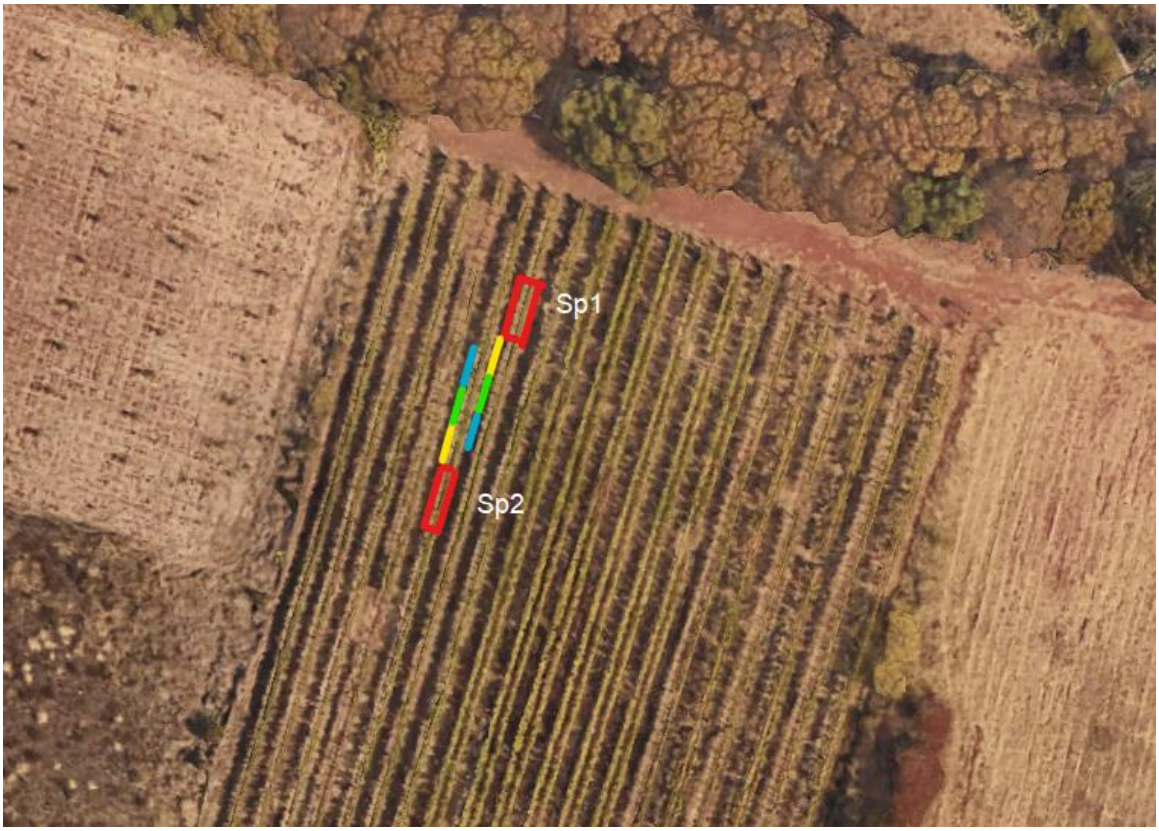

Figure 10. Representation of the SPs in the vineyard.

3.6. Image analysis

The image analysis performed in this work divided in three separate datasets:, and manual lab images (1), manual field images (2) and Vinbot field images (3). All images were collected during the 2019 season by the ISA research team (Samà, 2019). Each dataset was collected in different conditions and encompassed a total of 103, 90 and 120 images, respectively. In all three datasets, the number of visible berries on the images was counted using a program developed in MATLAB (R2010b, The Mathworks, Natick, MA, USA) to facilitate this laborious task. The program tracks the berries already counted and provides a sum of all counts in the end. The counting was performed manually without the aid of an automatic berry–segmentation algorithm (Aquino et al., 2018a), simply by clicking each berry in the image, thus producing an estimate of visible berries with the highest accuracy possible. In the following sections, the methodologies regarding each data set will be explained with detail.

3.6.1. Manual lab dataset

Of the 5 meters of carry length referred in the section 3.5. at each phenological stages, one representative segment was selected and all bunches from that segment were individually picked, packed and labelled to be analyzed in laboratory conditions. A total of 35 bunches were analyzed at each phenological stage. In the lab, bunches were photographed using the same manual RGB camera. To maintain the same distance from the bunch, the camera was mounted on a tripod in marked positions on the floor and moved to take two pictures in two different perspectives, front (side A) and side (side B). The bunches were hung on a bar with the use of a metal spring paper clip. A blue background was used to facilitate image analysis and remove background noise. Of the resulting images, the number of berries was estimated as explained above (section 3.5.). All methods related to estimating bunch area are described in Samà (2019). By ISA research team during 2019, bunches and berries were weighted in the laboratory using a KERN scale (KERN FCB Version 1.4) and the bunch volume was calculated by using the water displacement method (Samà, 2019).

In addition, in order to analyze individual berry weight and size and to estimate the berry growth factor during the vine growing cycle of grapes 2019, bunches were destemmed. The berries of each bunch were placed on a table and photographed. Afterwards, images were analyzed using the software ImageJ to automatically count the total number of berries for each bunch. (Bonaria, 2019; Samà, 2019).

In this study, images taken from the two perspectives (side A and B) of each bunch were analyzed using the MATLAB program described in section 3.5, to count the number of visible berries measured at bunch level (Vb_B) (*Fig. 11)*. For each phenological stage, the average Vb_B was calculated as the mean of visible berries from side A and side B, for each bunch. Using the actual berry number, we also obtained the percentage of Vb_B, in order to analyze the berry-by-berry occlusion measured at bunch level (AbO_B), obtained with the equation 7:

AbO_B (%) = 100 - average Vb_B (%) *Equation 7*

In addition, it was calculated the berry weight (bW) through the ratio between the bunch weight (BW) and the number of total berry measured in laboratory (Tb_L) of every single bunch (equation 8).

bW (g) = BW (g) / Tb_L *Equation 8*

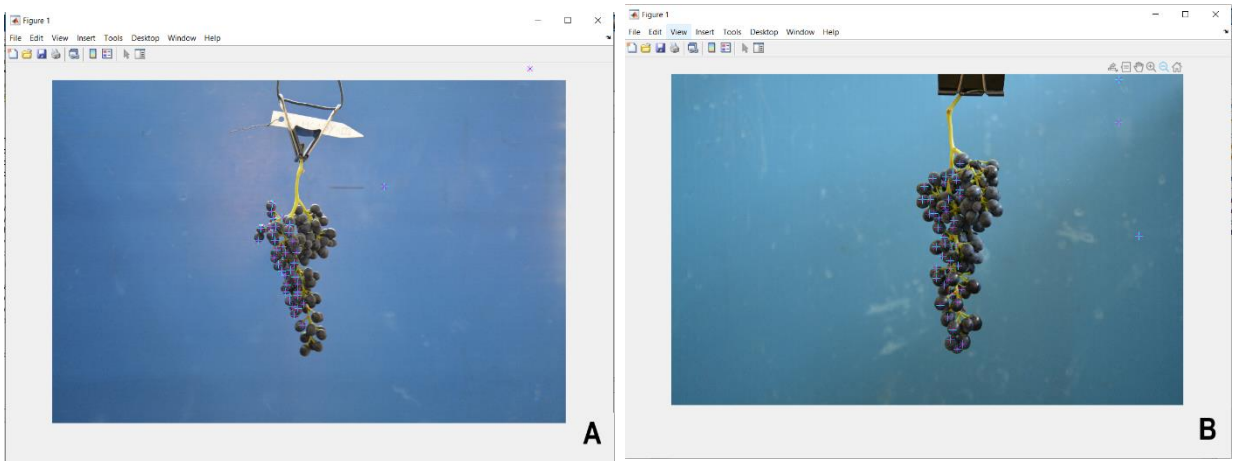

Figure 11. Counting the number of Syrah berries from side a (A) and side b (B) at the harvest phenological stage using MATLAB.

3.6.2. Manual field dataset

Images were collected in the vineyard with a commercial Nikon D5200 RGB camera during three phenological stages: pea size, veraison and maturation in the four smartpoints. As explained above, for each smartpoint, it was considered 5 meters of the canopy, these were analyzed at three different cluster zone defoliation levels (*Fig.* 12):

- Non-defoliated canopy
- Canopy partially defoliated
- Canopy completely defoliated.

Figure 12. Representation of the same vines, at three different levels of fruit zone defoliation at the stage of maturation (without any defoliation (A), partial defoliation (B), full defoliation (C) (Samà, 2019).

The photos were taken before and after the defoliation using a blue background. On each RGB image the number of visible berries was evaluated at different levels of defoliation and added to the data base which already included canopy porosity, occlusion and bunch area (Bonaria, 2019; Samà, 2019). The percentage of visible berries at vine level (Vb_v) was then calculated using the equation 9:

*Vb_v (%) = (#Visible berries at each defoliation levels / #Visible berries at total defoliation) * 100*

Equation 9

The main intention of this methodology is to simulate different canopy porosity or canopy gaps realities, that increase fruit exposure (Diago et al., 2016). In addition, relate that trait with the percentage of Vb_v. Vb_v is expected to increase with lesser amount of leaves (Aquino et al., 2018a).

3.6.3. Vinbot field dataset

RGB images were obtained by the Vinbot in field conditions only in one side of the row, controlling the robot position at a distance around 70 cm from the canopy and aligning it with the measuring tape located under the vines. A blue background was place on the opposite side of the row to aid future image analysis and prevent background noise from adjacent rows. The robot was piloted using a wireless joystick system, since its self-navigation system is still under development. In addition, a smartphone was used to communicate with Vinbot through Wi-Fi and to manage images collections. At the end of maturation, all grape bunches were harvested from the analyzed vine segments and the final yield was obtained for each segment. On each images captured, several canopy and bunch attributes were estimated using image analysis, such as bunch projected area in the images and canopy porosity (Samà, 2019) and were used in this work for further evaluation. In the same images, berries were counted manually as described in section 3.5. Yield was estimated on images of non-defoliated vines, collected by the Vinbot platform (*Fig.13*).

Figure 13. An example of Vinbot field image.

Yield estimation was performed using a combination of two models developed with both field data (manual field images) and laboratory data (manual lab images). The first model estimates the percentage of Vb_v that are being occluded by vegetation (equations 9-10-11):

*Vb_v (%) (pea-size) = - 0,017 * (P %)* ^{2} *+ 2,633 * (P %)* *Equation 10*

*Vb_v (%) (veraison) = - 0,017 * (P %)* ^{2} *+ 2,601 * (P %)* *Equation 11*

*Vb_v (%) (maturation) = 26,304 * ln(P %) - 11,844* *Equation 12*

They were obtained from linear regression between the porosity (%) and the Vb_v (%), for each phenological stage. The final result of these models represents the estimated total number of berries (Vbtot) that would be visible if all leaves were removed with the following equation:

*Vbtot = (Vb_v / Vb_v %) * 100* *Equation 13*

Where VB_v are the visible berries counted through MATLAB software. Therefore, this result does not yet include the total number of berries as many are still being occluded by neighboring berries. In order to estimate those fruits, a second model (2) was used to estimate the total number of berries (btot) based on Vbtot from a 2D perspective:

*btot (pea-size) = 1,073 **Vbtot + *1,973* *Equation 14*

*btot (veraison) = 1,325 **Vbtot - *7,984* *Equation 15*

*btot (maturation) = 1,749 **Vbtot - *15,590* *Equation 16*

After applying both models BT_{LB} is then multiplied by the average bW (also estimated with a sample from laboratory data), in order to obtain the estimated yield:

*Yest (kg) = (btot * bW (g)) / 1000* *Equation 17*

Yest was then compared with actual yield (Y), with the aim of achieving the percentage of error (E%).

*E% = (Yest - Y)(kg) / Y (kg)) * 100* *Equation 18*

3.7. Data analysis

In each dataset and for all the phenological stages (pea-size, veraison and maturation), data was analyzed using different statistical test in Microsoft Excel. One-way ANOVA was employed in lab dataset to compare the effect of the different bunch image perspectives of Vb_B side A and Vb_B side B. Correlation and regression analysis were used to assess the relationships between variables.

4. RESULTS AND DISCUSSION

4.1. Laboratory results

The table 1 shows some average values between SP1 and SP2, obtained from the data collected in laboratory during pea-size, veraison and harvest. Regarding BW, bW and AbW, cv. Syrah presents the highest values at maturation. According with Victorino et al., (2020) this was caused from an increase of the size of bunches and consequently of berries during the growing cycle of the bunch. In fact, as table shows, ABV is higher in maturation than in the other phenological stages. On the other hand, Vb_B side A, Vb_B side B and average Vb_B values decreased, due to the increase of ABV and AbO_b. These later values influence the berries visibility due to the occlusion berry-by-berry. Instead, regarding Tb_L (estimated using ImgageJ software by ISA 2019 team) no statistical differences were identified among phenological stages. In fact, althought the averages are different, the standard deviation shows that it was casually; therefore the number of berries is the same.

Table 1. Minimum value (Min), average ± standard deviation (Avg) and maximum value (Max.), of bunch and berry attributes, at pea size (n=35), veraison (n=33) and maturation (n=35), for each bunch of the cv Syrah. The variables are: bunch weight (BW), berry weight (bW), average berry weight (AbW), total berry number counted in laboratory condition (Tb_L), visible berries side A (Vb_B side A), visible berries side B (Vb_B side B), average number of visible berries (Vb_B), % of visible berries in laboratory condition (Vb_L), percentage of the average berry-by-berry occlusion (AbO_b) and actual bunch volume (ABV).

Bunch and berry attributes	**PEA-SIZE**			**VERAISON**			**MATURATION**		
	Min	**Avg**	**Max**	**Min**	**Avg**	**Max**	**Min**	**Avg**	**Max**
BW (g)	2.7	13.8 ± 8.2	35.6	8.7	33.9 ± 17.5	83.3	4.9	57.6 ± 29.5	145
bW (g)	2.5	11.5 ± 7.1	31.3	6.7	30.4 ± 16.1	73.1	3.7	54.1 ± 27.7	135.7
AbW (g)	0.1	0.2 ± 0.05	0.3	0.2	0.5 ± 0.1	0.2	0.2	0.8 ± 0.2	1.2
Tb_L	22	67 ± 31.5	148	22	63.7 ± 23.4	123	20	67.9 ± 38	212
Vb_B side A	21	59.7 ± 27.4	139	21	52.4 ± 16.6	81	20	48.5 ± 23.4	136
Vb_B side B	22	60.9 ± 26.2	120	22	55.7 ± 18.9	108	19	46.3 ± 18.7	100
Average Vb_B	21.5	60.3 ± 26.5	129.5	21.5	53.7 ± 17.5	92.5	19.5	47.8 ± 20.9	118
Vb_L (%)	32.4	94.3 ± 26	228.1	70	85.8 ± 7.2	97.7	50.5	74.9 ± 11.4	97.5
AbO_b (%)	-	5.7 ± 74	-	-	14.2 ± 92.8	-	-	25.1 ± 88.6	-
ABV (ml)	2.5	11.9 ± 8.5	35	5	31.8 ± 17	80	5	51.9 ± 27.8	135

4.1.1. Effect of bunch side on visible berry number

The one-way ANOVA Test analysis was carried out to compare visible berries between side A and side B in pea-size, veraison and maturation. In all of phenological stages F test was greater than 5% consequently the null hypothesis can be accepted. Therefore, there are no significant differences between visible berries on side A as compared to side B. For this reason, in data analysis have not been taken in consideration Vb_B side A and Vb_B side B but their average (average Vb_B).

4.1.2. Laboratory correlation analysis

Table 2 shows correlation coefficients (r) between bunch data of the cultivar Syrah, measured at pea-size, veraison and maturation. All the relationships present a high and positive r, therefore an increase in the independent variable corresponds to an increase in the dependent variable. Correlation coefficient between Tb_L and BW is high and constant in the three phenological stages. Instead, the correlation between average Vb_B and BW is highest in veraison as well as the relationship between average Vb_B and Tb_L. The good correlations suggest that these variables can be used as explanatory variables to estimate grapevine yield. In fact, in according with Clingeleffer (2001), Nuske et al., (2011a) and Nuske et al., (2014b) Tb_L and Vb_B are good explanatory of bunch weight. For this reason, many authors to estimate yield used these variables (Diago et al., 2014; Herrero-Huerta et al., 2015; Lopes et al., 2017; Aquino et al., 2018a; Zabawa et al., 2019; Santos et al., 2020; Coviello et al., 2020; Liu et al., 2020b).

Table 2. Correlation coefficient between variables of cultivar Syrah. Values are: bunch weight (BW), total berry number (Tb_L) and average number of visible berries (Average Vb_B). The *** indicates the significance at P≤0.001

Bunch and berry attributes	**PEA-SIZE**			**VERAISON**			**MATURATION**		
	BW (g)	Tb_L	Average Vb_B	BW (g)	Tb_L	Average Vb_B	BW (g)	Tb_L	Average Vb_B
BW (g)	1	-	-	1	-	-	1	-	-
Tb_L	0.91***	1	-	0.91***	1	-	0.89***	1	-
Average Vb_B	0.82***	0.90***	1	0.87***	0.98***	1	0.85***	0.96***	1

4.1.3. Relationship between average number of visible berry and bunch weight

It was calculated the relationship between the average Vb_B (independent variable) and the BW (dependent variable) of bunches, obtaining respectively the following determination coefficient for each phenological stage: R^2=0.68 at pea-size (*Fig. 14A*), R^2=0.78 at veraison (*Fig. 14B*) and R^2=0.71 at maturation (*Fig. 14C*). These regression analyses, showed a high and significant coefficient of determination, indicating that the average Vb_B is a good estimator of BW especially at veraison.

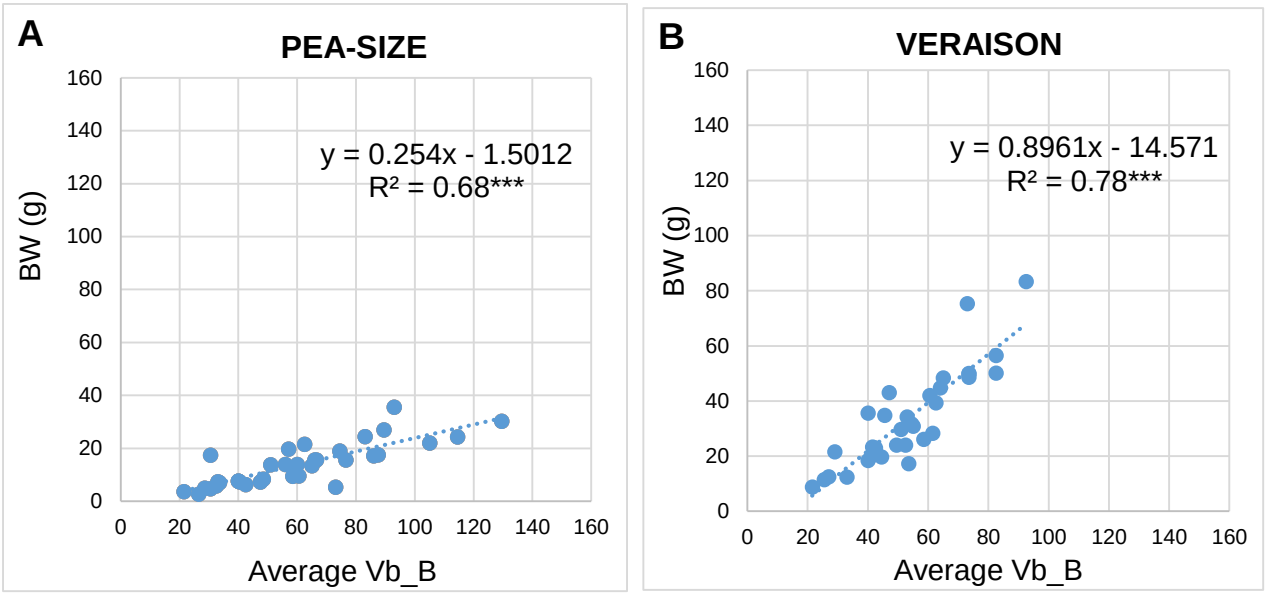

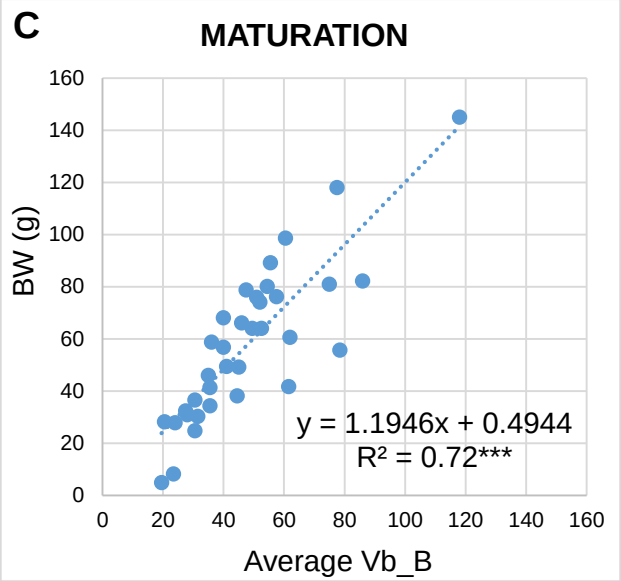

Figure 14. Linear regression analysis between average number of visible berries (average Vb_B) (independent variable) and bunch weight (BW) (dependent variable) at pea-size (A) (n=35), veraison (B) (n=33) and maturation (C) (n= 35). The *** indicates the significant R^2 at p≤0.001.

4.1.4. Relationship between average number of visible berries and total number of berries

The relationship between the average Vb_v (independent variable) and the Tb_L (dependent variable) shows the coefficient of determinations different for each phenological stage. These values of R^2 was 0.80 at pea-size (*Fig. 15A*), 0.96 at veraison (*Fig. 15B*) and 0.93 at maturation (*Fig. 15C*). The linear regression analysis showed highly significant results for the three phenological stages, therefore the average Vb_B is a good explanatory of the Tb_L variability. These results are in according with values obtained in other studied such as Grossetete et al., (2012); Herrero-Huerta et al., (2015) and Aquino et al., (2017).

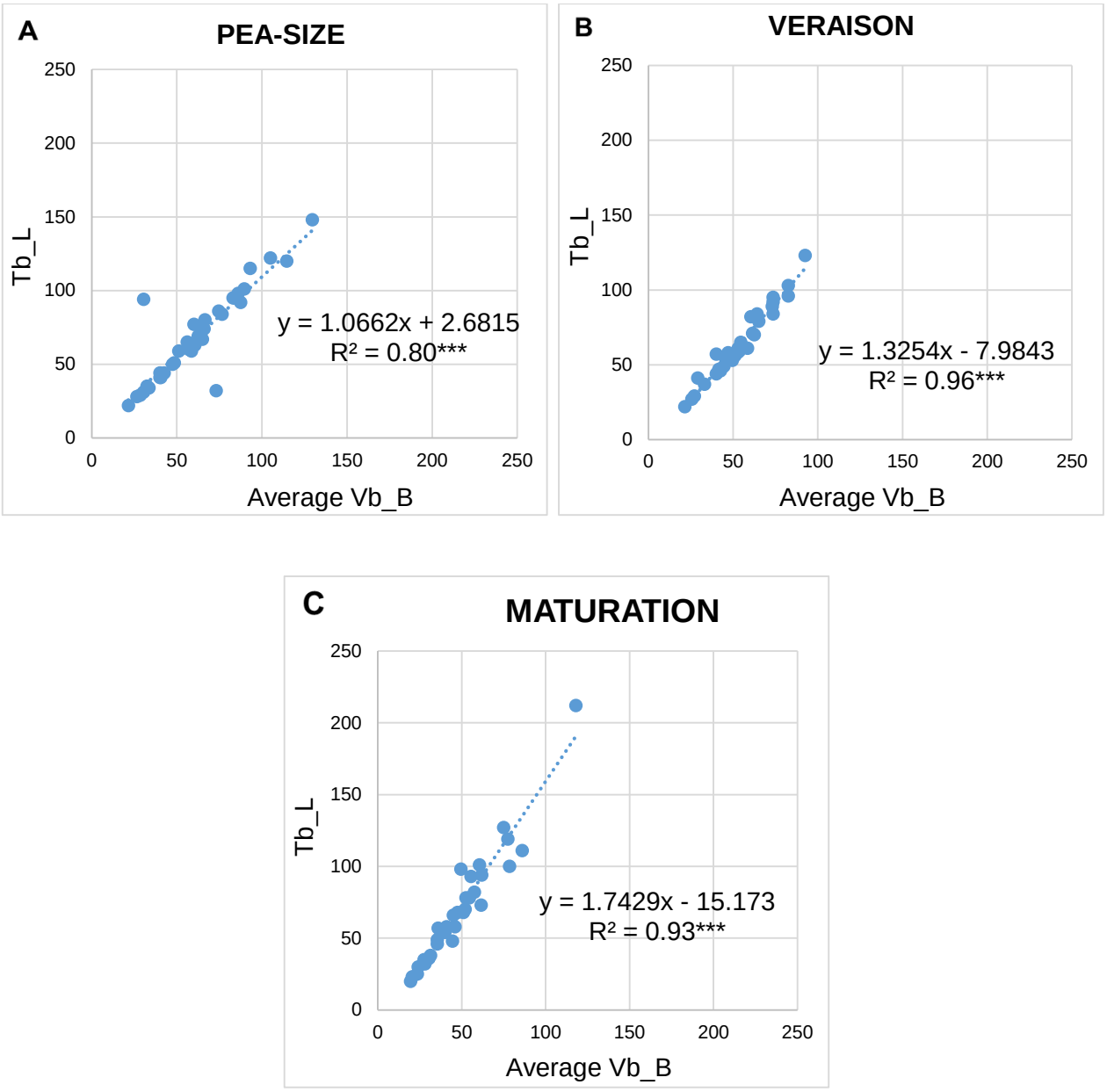

Figure 15. Linear regression analysis between average number of visible berries (average Vb_B) (independent variable) and total number of berries (Tb_L) (dependent variable), at pea-size (A) (n=35), veraison (B) (n=33) and maturation (C) n= 35. The *** indicates the significant R^2 at p≤0.001.

4.2. Field manual images

Table 3 presents the percentage of canopy porosity, the Visble Bunch Area (VBA) (estimated using ImageJ software) and the percentage of Vb_v, for each phenological stages at different level of defoliation.

The results show that as defoliation level increases, the percentage of porosity and the percentage of Vb_v increase. In this way, there were more gaps, which expected and explained the higher visibility of the berries (Diago et al., 2016). Regarding the percentage of Vb_v identified through MATLAB were higher than in the other phenological stages in each defoliation degree. This is due to the increase of the bunch size and consequently of the VBA during the phenological stages. In addition, the Table 3 shows, in non-defoliation condition, the increasing of Vb_v during the growing cycle of the bunch due to VBA increased. Yet, this can be also caused by the water stress, since the plot variety was not irrigated that led to an increase of leaf senescence and the canopy porosity % (Victorino et al., 2020).

Table 3. Average values ± standard deviation of the canopy porosity (%), visible bunch area (VBA) and the % of the visible berries at vine level (Vb_v) at different level of defoliation, during pea-size (n=30), veraison (n=30) and maturation (n=30).

Defoliation degree	**PEA-SIZE**			**VERAISON**			**MATURATION**		
	P (%)	VBA (cm^2)	Vb_v (%)	P (%)	VBA (cm^2)	Vb_v (%)	P (%)	VBA (cm^2)	Vb_v (%)
No	7.9 ± 3.3	68.9 ± 37.6	18.9 ± 8.3	8.1 ± 4.1	100 ± 70.1	19.4 ± 9	13.7 ± 3.4	242.9 ± 130.2	56 ± 18.1
Partial	15.1 ± 6.1	132.7 ± 56.8	40.7 ± 14.1	15.7 ± 5	190 ± 107.8	38.4 ± 10.5	21 ± 5.8	341.7 ± 165.8	66.9 ± 19
Total	74.4 ± 3.2	282 ± 79.7	100	69.7 ± 5.3	477 ± 199.2	100	67.8 ± 5.5	538.5 ± 122.5	100

4.2.1. Correlation analysis

Table 4 shows correlation coefficients (r) between variables obtained from manual field images at pea-size, veraison and maturation.

The correlation between porosity % and Vb_v is very high in all the phenological stages but the lowest value was recorded at maturation as well as in the relationship between the percentage of Vb_v and porosity %. Regarding the correlation between the VBA and the porosity, the coefficient r is positive but decreases during the phenological stages and highest value was recorded at pea-size.

The actual yield (Y) presents a positive correlation coefficient with Vb_v at pea-size, veraison and maturation. This means that, with or without defoliation, the visible berries explain, to some extent, the final yield on manual field images. However, the r values are not very high, therefore to perform a yield estimation, it is necessary considering other variables.

Table 4. Correlation coefficient between bunch and berry attributes of cultivar Syrah, at pea-size (n=30), veraison (n=30) and maturation (n=30) in field conditions. The variables are: average number of visible berries at vine level (Vb_v), percentage of canopy porosity (P %), visible bunch area (VBA) and actual yield (Y). The * indicates the significance at P≤0.1 The ** indicates the significance at P≤0.01 and *** indicates the significance at P≤0.001 and n.s. not significant.

Phenological stage	Bunch and berry attributes	Vb_v	P (%)	VBA	Vb_v (%)	Y
Pea-size	Vb_v	1	-	-	-	-
	P (%)	0.86***	1	-	-	-
	VBA	0.98***	0.81***	1	-	-
	Vb_v (%)	0.90***	0.95***	0.88***	1	-
	Y	0.31 n.s.	0.02 n.s.	0.38 *	0.03 n.s.	1
Veraison	Vb_v	1	-	-	-	-
	P (%)	0.76 ***	1	-	-	-
	VBA	0.89 ***	0.70 ***	1	-	-
	Vb_v (%)	0.82 ***	0.93 ***	0.78 ***	1	-
	Y	0.42 *	-0.10 n.s.	0.49 **	0.04 n.s.	1
Maturation	Vb_v	1	-	-	-	-
	P (%)	0.67 ***	1	-	-	-
	VBA	0.96 ***	0.66 ***	1	-	-
	Vb_v (%)	0.71 ***	0.79 ***	0.78 ***	1	-
	Y	0.61 ***	0.03 n.s.	0.66 ***	0.28 n.s.	1

4.2.2. Relationship between canopy porosity and the percentage of visible berries

For each phenological stages, the regression analysis between porosity % (independent variable) and the % Vb_v (dependent variable) was evaluated at different level of defoliation. These relationships show a R^2 of 0.88 at pea-size (*Fig. 16A*), 0.84 at veraison (*Fig. 16B*) and 0.63 at maturation (*Fig. 16C*). The polynomial (pea-size and veraison) and log (maturation) regressions show a high and significant determination coefficient indicating that the model can be used to

explain the % Vb_v variability covered by leaves. Nevertheless, a decrease in the R^2 was observed throughout the phenological phases, in particular a lower value was found at maturation, showing that, at this phenological stage, the visibility of the berries depends less on the porosity.

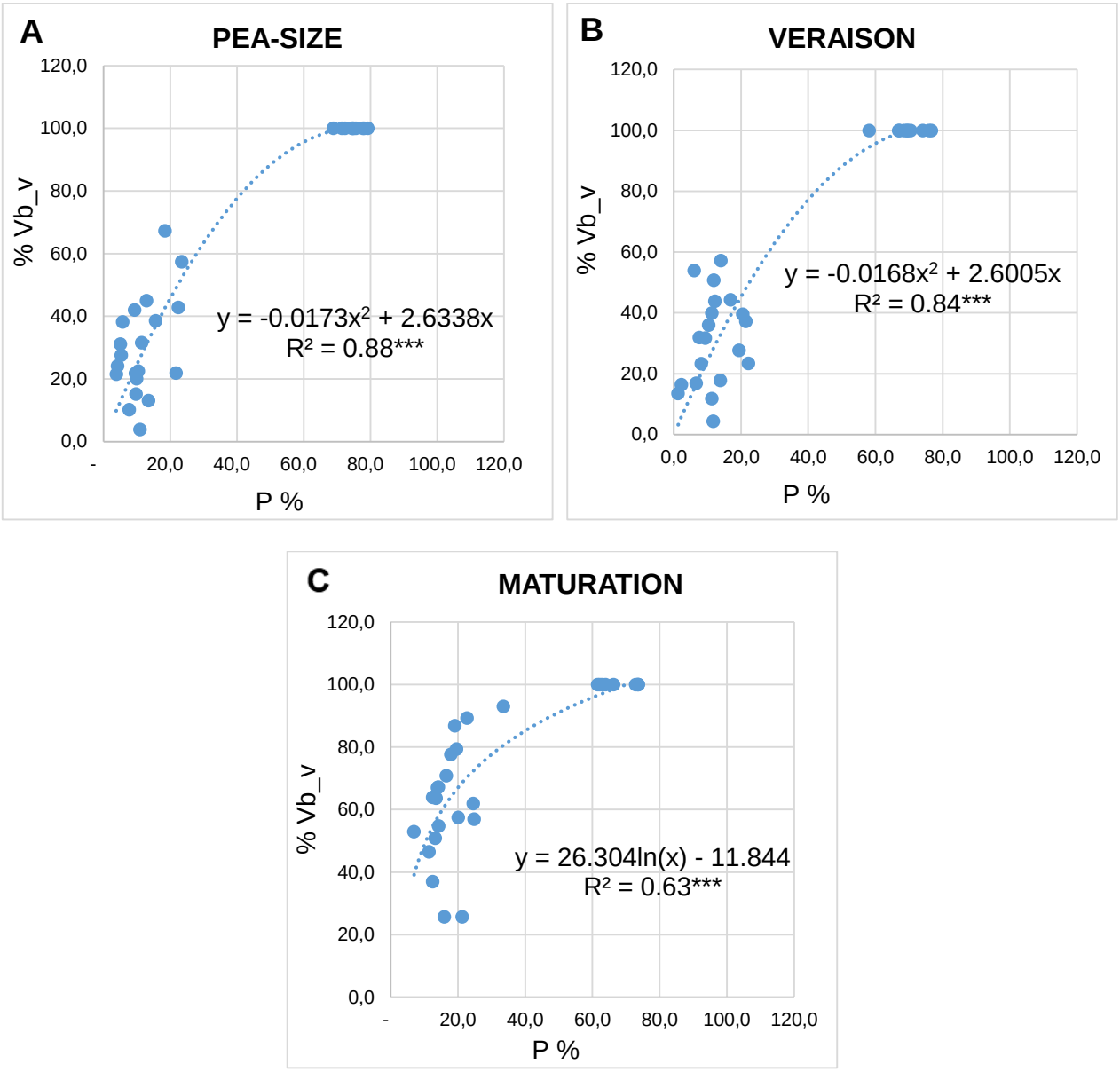

Figure 16. Relationship between the percentage of canopy porosity (P %) (Independent variable) and the percentage of visible berries (% Vb_v) (dependent variable), polynomial and log regression equations and coefficient R^2, at pea-size (A) (n=30), at veraison (B) (n=30) and at maturation (C) (n=30). The *** indicates the significant R^2 at p≤0.001.

4.2.3. Relationship between number of visible berries and actual yield

For each phenological stages it was studied the relationship between the Vb_v (independent variable) and Y (dependent variable) explained in the linear regressions. Graphs show high and significant determination coefficients, respectively 0.60 at pea-size (*Fig. 17A*), 0.68 at veraison (*Fig. 17B*) and 0.61 at maturation (*Fig.17C*).

Determination coefficients were constant in all of the phenological stages, probably because the relationship was analyzed taking in consideration the variables in total defoliation condition. In this way there was not the occlusion by leaves, but only the berry-by-berry occlusion. Therefore the Vb_v are a good explanatory of the Y variability.

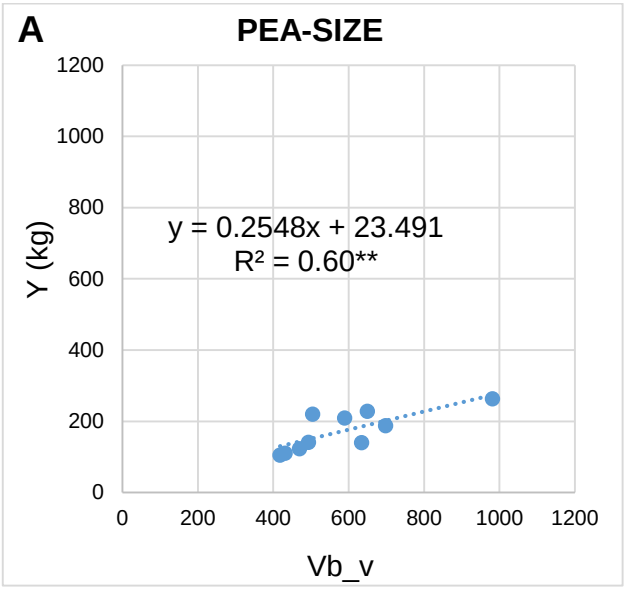

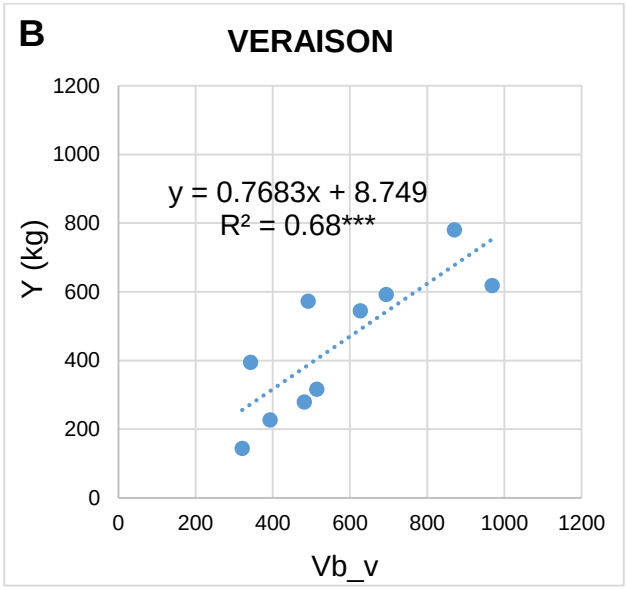

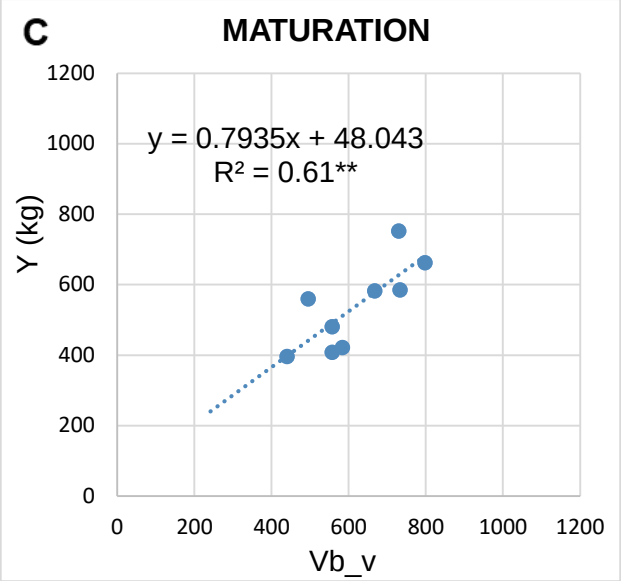

Figure 17. Relationship between visible number of berries (Vb_v) (independent variable) and actual yield (Y) (dependent variable), linear regression equations and coefficient R^2, at pea-size (A) (n=30), veraison (B) (n=30) and maturation (C) (n=30). The ** indicates the significant R^2 at p≤0.01 and *** indicates the significant R^2 at p≤0.001.

4.3. Vinbot results

Table 5 presents average values of bunch and berry attributes obtained from images taken with the VINBOT platform, during pea-size, veraison and maturation in field condition.

Vb_v and % Vb_v were more detected in maturation than in other phenological stage. This is due to an increase of the canopy porosity % during the phenological stages that makes bunches more visible. According with Victorino et al., (2020) study, VBA increased during the growing cycle of the vine and this is another variable increasing bunches visibility. Regarding Vbtot the lowest value was recorded at maturation stage, this means that without the occlusion by leaves, the decrease of berries visibility was due to the occlusion by other berries. In fact, btot without leaves and berry-by-berry occlusion was higher during veraison and maturation than in pea-size. Instead Yest retained a constant value during the three phenological stages.

Table 5. Minimum value (Min), average ± standard deviation (Avg) and maximum value (Max.), of bunch and berry attributes, at pea size (n=40 vine segments), veraison (n=40 vine segments) and maturation (n=40 vine segment). The variables are: number of visible berries at vine level (Vb_v), % of canopy porosity (P%), visible bunch area (VBA), % of visible berries (%Vb_v), total number of visible berries without leaves occlusion (Vbtot), total number of visible berries without berries and leaves occlusion (btot) and yield estimate (Yest).

Bunch and berry attributes	**PEA-SIZE**			**VERAISON**			**MATURATION**		
	Min	**Avg**	**Max**	**Min**	**Avg**	**Max**	**Min**	**Avg**	**Max**
Vb_v	10	94.3 ± 43.4	191	21	117.2 ± 66.6	299	25	196 ± 105	491
P (%)	3	9.6 ± 4.5	22	3.6	12.1 ± 5.9	27.4	5.4	16 ± 5.8	30.4
VBA (cm^2)	5	80.6 ± 51.7	216.9	7.9	130.4 ± 77.5	342.9	44.7	222.1 ± 189.7	497.5
% Vb_v	7.7	23.3 ± 10.2	49.6	9.2	28.4 ± 12.5	58.7	32.4	59.4 ± 9.9	77.9
Vbtot	31.9	457 ± 264.8	1374.5	67.5	507.3 ± 400	1824.7	73.6	364.3 ± 148.8	705
btot	36.7	489.9 ± 282.3	1468.2	81.5	664.4 ± 530	2410.5	113.1	619.8 ± 259.4	1213.5
Yest (kg/m)	0	0.4 ± 0.23	1.2	0.1	0.5 ± 0.43	2	0.1	0.5 ± 0.2	1

In table 6, for each phenological stages, it was compared the Yest and the Y of all the bunches identified with MATLAB. Regarding the estimated total yield the lowest value was recorded in pea-size, while between veraison and maturation the value retained constant. In all of the phenological stages errors was negative, this means that Yest was underestimated during the growing cycle of bunches. High errors can be attributed to the failure of cultural operations such as cluster thinning and defoliation, leading to the cover of bunches by other bunches or by leaves. The minimum value of %E occurs at veraison stage, this was predictable since the highest btot value (table 5) was obtained in this phenological stage.

Table 6. Estimated yield (Yest), actual yield (Y) and the error (E %) between them at pea-size (n=40 vine segments), veraison (n=40 vine segments) and maturation (n=40 vine segments).

Phenological stage	**Yest (kg/40m)**	**Y (kg/40m)**	**E (%)**
Pea-size	16.03	32.6	-51
Veraison	21.7	32.6	-33.3
Maturation	20.3	32.6	-37.8

In the Figure 18, actual and estimated yield are compared for each meter at maturation stage. In general the estimated yield presents a similar trend to actual yield. However, in several vine segments, yield was underestimated. According with Lopes et al., (2016), this can be due to bunches occluded by other bunches that might be influenced of the number and size of bunches. In Nuske et al., (2011b) were proposed two methods to overcome the bunch occlusion problem through the calibration of bunch occlusion ratio. However, Yest was overestimated in segments 12, 21 and 26. A possible explanation is that, because the model estimates the total berries considering the porosity, peak overestimation of yield happen in cases of low porosity and high berry visibility.

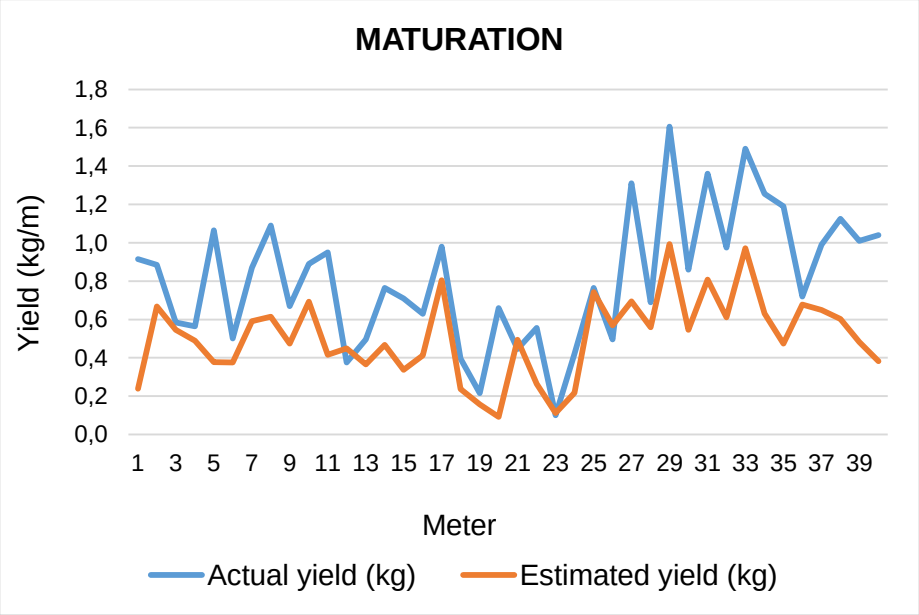

Figure 18. Actual and estimated results of yield per meter, at maturation (n=40 vine segment).

5. CONCLUSIONS

The main objective of this work was to estimate vineyard yield by counting the number of visible berries in images obtained in the frame of Vinbot project, at three phenological stages during the 2019 season. Data obtained in laboratory showed a high correlation between average number of visible berries and bunch weight, indicating a higher association between the two variables especially at veraison stage. The linear regression between the average number of visible berries and total berry number presented the highest determination coefficient at veraison, indicating that the average number of visible berries is a strong explanatory variable of total berry number. The relationship between canopy porosity and number of visible berries showed also high determination coefficient, with the lowest value recorded at maturation, indicating that the berries visibility is less influenced by porosity at maturation than at the other phenological stages. The linear regression between actual yield and number of visible berries presented a high and significant determination coefficient at all the three phenological stages. The berry-by-berry occlusion presented the highest value at maturation and the lowest one at pea-size. Finally, yield was estimated, using a regression model that estimate non-visible berries using canopy porosity as explanatory variable, combined with the average berry weight determined at harvest. The comparison of estimated yield with actual yield, showed an underestimation at all the three phenological stages. This low accuracy of the developed models show that the use of algorithms based on visible berry number on the images to estimate yield still needs further research.

6. REFERENCES

Aquino, A., Barrio, I., Diago, M., Millan, B., & Tardaguila, J. (2018a). vitisBerry : An Android-smartphone application to early evaluate the number of grapevine berries by means of image analysis. Computers and Electronics in Agriculture, 148(February), 19–28.

Aquino, A., Millan, B., Diago, M. P., & Tardaguila, J. (2018b). Automated early yield prediction in vineyards from on-the-go image acquisition. Computers and Electronics in Agriculture, 144, 26–36.

Aquino, A., Diago, M. P., Millán, B., and Tardáguila, J. (2017). A new methodology for estimating the grapevine-berry number per cluster using image analysis. Biosystems engineering, 156, 80–95.

Aquino, A., Millan, B., Gutiérrez, S., Tardáguila, J. (2015). Grapevine flower estimation by applying artificial vision techniques on images with uncontrolled scene and multi-model analysis. Computers and Electronics in Agriculture, 119, 92–104.

Behroozi-Khazaei, N., Maleki, M.R. (2017). A robust algorithm based on color features for grape cluster segmentation. Computers and electronics in agriculture, 142, 41–49.

Blom, P. E., & Tarara, J. M. (2009). Trellis tension monitoring improves yield estimation in vineyards. HortScience, 44, 678–685.

Bonaria, R., (2019). Grapevine yield estimation using image analysis for the variety Arinto. Master Thesis. Instituto Superior de Agronomia – Universidade de Lisboa.

Brancadoro, L., & Carnevali, P. (2010) Proximal sensing per la viticoltura sito-specifica. Valutazione multiscala delle potenzialità enologiche del vigneto. Relazione Scientifica. Dipartimento di Produzione Vegetale - Università degli studi di Milano.

Breviglieri, N., & Casini, E. (1962) Syrah. Principali vitigni da vino coltivati in Italia. Volume II. Ministero dell'Agricoltura e delle Foreste. Roma, Italy.

Clingeleffer P.R., Martin S.R., Dunn G.M. and Krstic M.P., 2001. Crop Development, Crop Estimation and Crop Control to Secure Quality and Production of Major Wine Grape Varieties: A National Approach. CSIRO and NRE: Victoria, Australia.

Cortez, R., Luna-Vital, D. A., Margulis, D., & Gonzalez de Mejia, E. (2017). Natural pigments: stabilization methods of anthocyanins for food applications. Comprehensive Reviews in Food Science and Food Safety, 16(1), 180-198.

Cosmo, I., Comuzzi, A., & Polsinelli, M. (1958). Portinnesti della vite. Edizioni Agricole, Bologna. 172.

Cotton, S. (1996). Colour, colour spaces and the human visual system. University of Birmingham, School of Computer Science. Technical Report.

Coviello, L., Cristoforetti, M., Jurman, G., & Furlanello, C. (2020). GBCNet: In-field grape berries counting for yield estimation by dilated CNNs. Applied Sciences (Switzerland), 10(14).

Cristofolini, F., & Gottardini, E. (2000). Concentration of airborne pollen of Vitis vinifera L. and yield forecast: A case study at S. Michele all'Adige, Trento, Italy. Aerobiologia, 16, 125–129.

Cunha, M., Abreu, I., Pinto, P., & Castro, R. De. (2003). Airborne Pollen Samples for Early-Season Estimates of Wine Production in a Mediterranean Climate Area of Northern Portugal. 3(January), 189–194.

Diago, M. P., Aquino, A., Millan, B., Palacios, F., & Tardaguila, J. (2019). On-the-go assessment of vineyard canopy porosity, bunch and leaf exposure by image analysis. Australian Journal of Grape and Wine Research, 25, 363–374.

Diago, M. P., Correa, C., Millán, B., Barreiro, P., Valero, C., & Tardaguila, J. (2012). Grapevine yield and leaf area estimation using supervised classification methodology on RGB images taken under field conditions. Sensors (Switzerland), 12, 16988–17006.

Diago, M. P., Krasnow, M., Bubola, M., Millan, B., & Tardaguila, J. (2016). Assessment of vineyard canopy porosity using machine vision. American Journal of Enology and Viticulture, 67, 229–238.

Diago, M. P., Sanz-Garcia, A., Millan, B., Blasco, J., & Tardaguila, J. (2014). Assessment of flower number per inflorescence in grapevine by image analysis under field conditions. Journal of the Science of Food and Agriculture, 94, 1981–1987.

Di Gennaro, S. F., Toscano, P., Cinat, P., Berton, A., & Matese, A. (2019). A low-cost and unsupervised image recognition methodology for yield estimation in a vineyard. Frontiers in Plant Science, 10(May)

Doutor, O., Manuel, C., & Lopes, A. (2018). Estimativa da produção de uva na casta Encruzado com recurso a análise de imagem José António Peixoto de Queiroz Dissertação para obtenção do grau de Mestre em Engenharia de Viticultura e Enologia. 17-21.

Dunn, G.M., & Martin, S.R. (2007). A functional association in Vitis vinifera L. cv. Cabernet Sauvignon between the extent of primary branching and the number of flowers formed per inflorescence. Australian Journal of Grape and Wine Research, 13, 95–100.

Dunn, G. M., Martin, S. R., Krstic, M. P., & Petrie, P. R. (2014). Better Yield Forecasting in Vineyards. Wine Australia. 30-85

Ferrandino, A., Pagliarani, C., Carlomagno, A., Novello, V., Schubert, A., & Agati, G. (2017). Improved fluorescence-based evaluation of flavonoid in red and white winegrape cultivars. Australian Journal of Grape and Wine Research, 23, 207–214.

Fernández, R., Montes, H., Salinas, C., Sarria, J., & Armada, M. (2013). Combination of RGB and multispectral imagery for discrimination of Cabernet Sauvignon grapevine elements. Sensors (Switzerland), 13, 7838–7859.

Font, D., Tresanchez, M., Martínez, D., Moreno, J., Clotet, E., & Palacín, J. (2015). Vineyard yield estimation based on the analysis of high resolution images obtained with artificial illumination at night. Sensors (Switzerland), 15(4), 8284–8301.

Fuentes, S., Bei, R. De, & Tyerman, S. D. (2008). Image analysis techniques applied to canopies, berries, plant tissues and leaves. International Conference of Agricultural Engineering. The University of Adelaide, School of Agriculture, Food and Wine, Plant Research Centre PMB 1 Glen Osmond, SA., Australia.

Fuentes, S., Poblete-Echeverría, C., Ortega-Farias, S., Tyerman, S., & de Bei, R. (2014). Automated estimation of leaf area index from grapevine canopies using cover photography, video and computational analysis methods. Australian Journal of Grape and Wine Research, 20, 465–473.

Gené-Mola, J., Gregorio, E., Auat Cheein, F., Guevara, J., Llorens, J., Sanz-Cortiella, R., Escolà, A., & Rosell-Polo, J. R. (2020). Fruit detection, yield prediction and canopy geometric characterization using LiDAR with forced air flow. Computers and Electronics in Agriculture, 168, 105-121.

Grossetete, M., Berthoumieu, Y., Da Costa, J.P., Germain, C., Lavialle, O., Grenier, G. (2012). Early estimation of vineyard yield: site specific counting of berries by using a smartphone. International Conference of Agricultural Engineering—CIGR-AgEng.

Hacking, C., Poona, N., Manzan, N., & Poblete-Echeverría, C. (2019). Investigating 2-D and 3-D proximal remote sensing techniques for vineyard yield estimation. Sensors (Switzerland), 19(17).

Hall, A., Lamb, D. W., Holzapfel, B., & Louis, J. (2002). Optical remote sensing applications in viticulture - A review. Australian Journal of Grape and Wine Research, 8, 36–47.

He, X., Cai, D., & Niyogi, P. (2006). Laplacian score for feature selection. In Advances in neural information processing systems, 18, 507-514.

Herrero-Huerta, M., González-Aguilera, D., Rodriguez-Gonzalvez, P., Hernández-López, D. (2015). Vineyard yield estimation by automatic 3D bunch modelling in field conditions. Computers and electronics in agriculture, 110, 17–26.

Higgins, J. J. (2003). Introduction to Modern Nonparametric Statistics. Pacific Grove, CA: Brooks/Cole.

IPMA, Instituto Português do Mar e da Atmosfera. Available at:

http://www.ipma.pt/pt/oclima/normais.clima/1971-2000/001/. Accessed April, 20, 2019

Kendall, M. G. (1946). The advanced theory of statistics. The advanced theory of statistics., (2nd Ed). Charles Griffin & Company Limited, London.

Komm, B., & Moyer, M. (2015). Vineyard Yield Estimation. Washington State University Extension. Publishing, Pullman, Washington. 1–11.

Kottek, M., Grieser, J., Beck, C., Rudolf, B., & Rubel, F. (2006). World map of the Köppen-Geiger climate classification updated. Meteorologische Zeitschrift, 15(3), 259-263.

Liu, S., Marden, S., & Whitty, M. (2013). Towards automated yield estimation in viticulture. Australasian Conference on Robotics and Automation, ACRA, 2–4.

Liu, S., Cossell, S., Tang, J., Dunn, G., & Whitty, M. (2017). A computer vision system for early stage grape yield estimation based on shoot detection. Computers and Electronics in Agriculture, 137,

Liu, S., Zeng, X., & Whitty, M. (2020a). A vision-based robust grape berry counting algorithm for fast calibration-free bunch weight estimation in the field. Computers and Electronics in Agriculture, 173(December 2019), 105360.

Liu, S., Zeng, X., & Whitty, M. (2020b). 3DBunch: A Novel iOS-Smartphone Application to Evaluate the Number of Grape Berries per Bunch Using Image Analysis Techniques. IEEE Access, 8, 114663–114674.

Lopes, C. M., Graça, J., Sastre, J., Reyes, M., Guzmán, R., Braga, R., Monteiro, A., & Pinto, P. A. (2016). Vineyard yeld estimation by VINBOT robot - preliminary results with the white variety Viosinho. Proceedings 11th Int. Terroir Congress. Jones, G. and Doran, N.(Eds.), 458-463. Southern Oregon University, Ashland, USA.

Lopes, C., Torres, A., Guzman, R., Graca, J., Reyes, M., Victorino, G., Braga, R., Monteiro, A., & Barriguinha, A. (2017). Using an unmanned ground vehicle to scout vineyards for non-intrusive estimation of canopy features and grape yield. 20th GiESCO International Meeting, 2, 16–21.

Martin, S., Dunstone, R., Dunn, G. (2003). How to forecast wine grape deliveries using grape forecaster excel workbook version 7. Australian Grape and Wine Research and Development Corporation, Adelaide, Australia, 100. 4-50.

Matese, A., & Di Gennaro, S. F. (2015). Technology in precision viticulture: A state of the art review. International Journal of Wine Research, 7, 69–81.

Millan, B., Aquino, A., Diago, M.P., Tardáguila, J. (2017). Image analysis-based modelling for flower number estimation in grapevine. Journal of the Science of Food and Agriculture, 97, 784–792.

Minaee, S., Boykov, Y., Porikli, F., Plaza, A., Kehtarnavaz, N., & Terzopoulos, D. (2020). Image Segmentation Using Deep Learning: A Survey. IEEE transactions on pattern analysis and machine intelligence. 1-23.

Nobuyuki, O., 1979. A threshold selection method from gray-level histograms. IEEE Trans Syst Man Cyb 9, 62–66.

Nuske, S., Achar, S., Bates, T., Narasimhan, S., & Singh, S. (2011a). Yield estimation in vineyards by visual grape detection. IEEE International Conference on Intelligent Robots and Systems, 2352–2358.

Nuske, S., Achar, S., Gupta, K., Narasimhan, S., & Singh, S. (2011b). Visual Yield Estimation in Vineyards: Experiments with Different Varietals and Calibration Procedures. CMU-RI-TR-11-39.

Nuske, S., Gupta, K., Narasimhan, S., & Singh, S. (2014a). Modeling and calibrating visual yield estimates in vineyards. Springer Tracts in Advanced Robotics, 92, 343–356.

Nuske, S., Wilshusen, K., Achar, S., Yoder, L., Narasimhan, S., & Singh, S. (2014b). Automated Visual Yield Estimation in Vineyards. Journal of Field Robotics, 31(5), 837–860.

Otsu, N. (1979). OTSU paper. IEEE Transactions on Systems, Man and Cybernetics, 20(1), 62–66.

Reyes, M., & Sastre, J., (2014). Report of the Computer Vision Algorithms, Data Process, System Specification, Evaluation and Results. Vinbot Autonomous Cloud-Computing Vineyard Robot to Optimize Yield Management and Wine Quality, 1-40.

VineGuard [homepage on the Internet]. Development of an Autonomous vineyard sprayer. Available from: http://robotics.bgu.ac.il/mw/index.php/Development_of_an_Autonomous_vineyard_sprayer. Accessed November, 11, 2020.

Rodríguez-Pulido, F. J., Gómez-Robledo, L., Melgosa, M., Gordillo, B., González-Miret, M. L., & Heredia, F. J. (2012). Ripeness estimation of grape berries and seeds by image analysis. Computers and Electronics in Agriculture, 82, 128–133.

Rosell Polo, J. R., Sanz, R., Llorens, J., Arnó, J., Escolà, A., Ribes-Dasi, M., Masip, J., Camp, F., Gràcia, F., Solanelles, F., Pallejà, T., Val, L., Planas, S., Gil, E., & Palacín, J. (2009). A tractor-mounted scanning LIDAR for the non-destructive measurement of vegetative volume and surface area of tree-row plantations: A comparison with conventional destructive measurements. Biosystems Engineering, 102, 128–134.

Rudolph, R., Herzog, K., Töpfer, R., & Steinhage, V. (2019). Efficient identification, localization and quantification of grapevine inflorescences and flowers in unprepared field images using Fully Convolutional Networks. Vitis - Journal of Grapevine Research, 58, 95–104.

Sabbatini, P., Dami, I., & Howell, G. S. (2012). Predicting Harvest Yield in Juice and Wine Grape Vineyards. Michigan State University Extension, November, 1–12.

Samà, G., (2019). Grapevine yield estimation using image analysis for the variety Syrah. Master Thesis. Instituto Superior de Agronomia - Universidade de Lisboa.

Santos, T. T., de Souza, L. L., dos Santos, A. A., & Avila, S. (2020). Grape detection, segmentation, and tracking using deep neural networks and three-dimensional association. Computers and Electronics in Agriculture, 170(August 2019), 105247.

Searcy, S. (2008). Precision farming: A new approach to crop management. Texas Agricultural Extension Service, The Texas A&M Univeristy, College Station, Texas, USA. 15-20.

Quattrocalici [homepage on the Internet] Available from: https://www.quattrocalici.it/vitigni/syrah/. Accessed November 11, 2020.

Sivakumar, M. V. K., Gommes, R., & Baier, W. (2000). Agrometeorology and sustainable agriculture. Agricultural and Forest Meteorology, 103, 11–26.

Tardaguila, J., Diago, M. P., Millan, B., Blasco, J., Cubero, S., & Aleixos, N. (2013). Applications of computer vision techniques in viticulture to assess canopy features, cluster morphology and berry size. Acta Horticulturae, 978, 77–84.

Tkalčič, M., & Tasič, J. F. (2003). Colour spaces - Perceptual, historical and applicational background. IEEE Region 8 EUROCON 2003: Computer as a Tool - Proceedings, A, (Vol. 1), 304–308.

Turner, D., Lucieer, A., & Watson, C. (2011). Development of an unmanned aerial vehicle (UAV) for hyper resolution vineyard mapping based on visible, multispectral, and thermal imagery. 34th International Symposium on Remote Sensing of Environment - The GEOSS Era: Towards Operational Environmental Monitoring.

Victorino, G. F., Braga, R., Santos-Victor, J., & Lopes, C. M. (2020). Yield components detection and image-based indicators for non-invasive grapevine yield prediction at different phenological phases. OENO One, 54(4), 833–848.

VINBOT [homepage on the Internet]. Valencia: Robotnik Automation SLL Available from: https://robotnik.eu/. Accessed November, 11, 2020.

VineRobot [homepage on the Internet].The VineRobot project coordinated by Televitis group, at the University of La Rioja in Spain. Available from: http://www.vinerobot.eu/. Accessed November,11, 2020

Vision Robotics [homepage on the Internet]. San Diego, CA: Vision Robotics Corporation (VRC). Available from: https://www.visionrobotics.com/. Accessed November, 11, 2020.

Vitirover [homepage on the Internet]. Saint-Émilion: Vitirover. Available from: https://www.vitirover.fr/en-home. Accessed November, 11, 2020.

Wall-ye [homepage on the Internet]. Available from: http://wall-ye.com/. Accessed November 11, 2020.

Whalley, J., & Shanmuganathan, S. (2013). Applications of image processing in viticulture: A review. 20th International Congress on Modelling and Simulation, December, 531–537.

Zabawa, L., Kicherer, A., Klingbeil, L., Milioto, A., Töpfer, R., Kuhlmann, H., & Roscher, R. (2019). Detection of single grapevine berries in images using fully convolutional neural networks. In Proceedings of the IEEE/CVF Conference on Computer Vision and Pattern Recognition Workshops. 1-9.

Zabawa, L., Kicherer, A., Klingbeil, L., Töpfer, R., Kuhlmann, H., & Roscher, R. (2020). Counting of grapevine berries in images via semantic segmentation using convolutional neural networks. ISPRS Journal of Photogrammetry and Remote Sensing, 164, 73–83.